

JET PROPULSION LABORATORY

SIRTF IPF REPORT

JPL ID502095

November 12, 2003

**SIRTF INSTRUMENT POINTING FRAME
KALMAN FILTER EXECUTION SUMMARY**

IPF RUN NUMBER: 502095

REPORT TYPE: IOC EXECUTION (FINE)

PRIME FRAME: MIPS_24um_center (95)

INFERRRED FRAMES: (96) (99) (100) (103) (104)

IPF TEAM

Autonomy and Control Section (345)

Jet Propulsion Laboratory

California Institute of Technology

4800 Oak Grove Drive

Pasadena, CA 91109

Contents

1 IPF EXECUTION SUMMARY	5
2 IPF INPUT FILE HISTORY	9
3 IPF EXECUTION RESULTS	12
3.1 IPF EXECUTION OUTPUT PLOTS	12
3.2 IPF OUTPUT DATA (IF MINI FILE)	38
3.3 IPF EXECUTION LOG	42
4 COMMENTS	45

List of Figures

1.1 A-priori and a-posteriori IPF frames	5
1.2 A-priori and a-posteriori IPF frames (ZOOMED)	8
2.1 Scenario Plot	9
2.2 Attitude file edit history	10
2.3 Centroid file edit history	10
2.4 Oriented Pixel Coords of Centroid Meas. Edited Centroids	11
3.1 TPF coords of measurements and a-priori predicts	14
3.2 Oriented Pixel Coords of measurements and a-priori predicts	14
3.3 Oriented (W,V) Pixel Coords of A-Priori Prediction Error Quiver Plot	15
3.4 A-priori prediction error (Science Centroids)	15
3.5 Oriented Pixel Coords of measurements and a-priori predicts (PCRS only)	16
3.6 Oriented Pixel Coords of measurements and a-priori predicts (Zoomed, PCRS only)	16
3.7 Oriented (W,V) Pixel Coords of A-Priori PCRS Prediction Error Quiver Plot	17
3.8 A-priori PCRS prediction error	17
3.9 IPF execution convergence, chart 1	18
3.10 IPF execution convergence, chart 2	18
3.11 Parameter uncertainty convergence	19
3.12 IPF parameter symbol table	19
3.13 KF parameter error sigma plots	20
3.14 LS parameter error sigma plot	20

3.15 KF and LS parameter error sigma plot	21
3.16 Oriented Pixel Coords of meas. and a-posteriori predicts	22
3.17 Oriented Pixel Coords of meas. and a-posteriori predicts (attitude corrected)	22
3.18 KF innovations with (o) and w/o (+) attitude corrections	23
3.19 Histograms of science a-posteriori residuals (or innovations)	23
3.20 A-Posteriori Science Centroid Prediction Error Quiver (Att. Cor.)	24
3.21 Normalized A-Posteriori Science Centroid Prediction Errors	24
3.22 KF innovations with (o) and w/o (+) attitude corrections (PCRS)	25
3.23 Histograms of PCRS a-posteriori residuals (or innovations)	25
3.24 A-posteriori PCRS Prediction Summary	26
3.25 A-posteriori PCRS Prediction (PCRS 1 Only)	27
3.26 A-posteriori PCRS Prediction (PCRS 2 Only)	27
3.27 A-Posteriori PCRS Prediction Errors Quiver (Att. Cor.)	28
3.28 Normalized A-Posteriori PCRS Prediction Errors	28
3.29 W-axis KF innovations and 1-sigma bound	29
3.30 V-axis KF innovations and 1-sigma bound	29
3.31 Array plot with (solid) and w/o (dashed) optical distortion corrections	30
3.32 Optical Distortion Plot: total (x5 magnification)	30
3.33 Optical Distortion Plot: constant plate scales (x5 magnification)	31
3.34 Optical Distortion Plot: linear plate scale (x5 magnification)	31
3.35 Optical Distortion Plot: gamma terms (x5 magnification)	32
3.36 Scan Mirror Chops	32
3.37 IPF Frame Reconstruction	33
3.38 Center Pixel Reconstruction	33
3.39 Estimated attitude corrections (Body frame)	34
3.40 Estimated attitude error sigma plot (Body frame)	34
3.41 Thermo-mechanical boresight drift (equiv. angle in (W,V) coords)	35
3.42 Thermo-mechanical boresight drift (equiv. angle in Body frame)	35
3.43 Gyro drift bias contribution (equiv. rate in (W,V) coords)	36
3.44 Gyro drift bias contribution (equiv. angle in (W,V) coords)	36
3.45 Gyro drift bias contribution (equiv. angle in Body frame)	37

List of Tables

1.1	IPF filter input files	6
1.2	IPF filter execution configuration	6
1.3	IPF filter execution mask vector assignment	6
1.4	IPF calibration error summary ([arcsec], 1-sigma, radial)	7
1.5	Science measurement prediction error summary (1-sigma)	7
1.6	IPF Brown angle summary	8
2.1	IPF input file begin and end times	9
2.2	IPF input file editing status	9
2.3	List of Removed Centroids (Original CA File Row Index)	11
2.4	List of Removed PCRS Centroids (Original CB File Row Index)	11
3.1	Table of figures I (IPF run)	12
3.2	Table of figures II (IPF run)	13
3.3	PCRS measurement prediction error summary	26

1 IPF EXECUTION SUMMARY

This report summarizes the SIRTF Instrument Pointing Frame (IPF) Kalman Filter execution associated with run file: RN502095. In particular, this Focal Point Survey calibrates the instrument: MIPS_24um_center (95), as part of the IOC Fine Survey. The main calibration results from the IPF filter execution have been documented in IF502095 typically stored in the mission archive DOM collection IPF.IF. This report only summarizes the main aspects of the run, and does not substitute for the full information contained in the IF file.

Section 1 summarizes the filter execution results. The filter configurations are tabulated in Table 1.2 and the mask vector assignments are tabulated in Table 1.3. A total of 33 state parameters are estimated in this run. The overall End-to-End pointing performances are tabulated in Table 1.4. The prediction residuals throughout the estimation processes are tabulated in Table 1.5. Section 3 summarizes resulting plots, a mini summary of the IF IPF output file, and the execution log. Section 4 captures the user comments that are specific to this particular run.

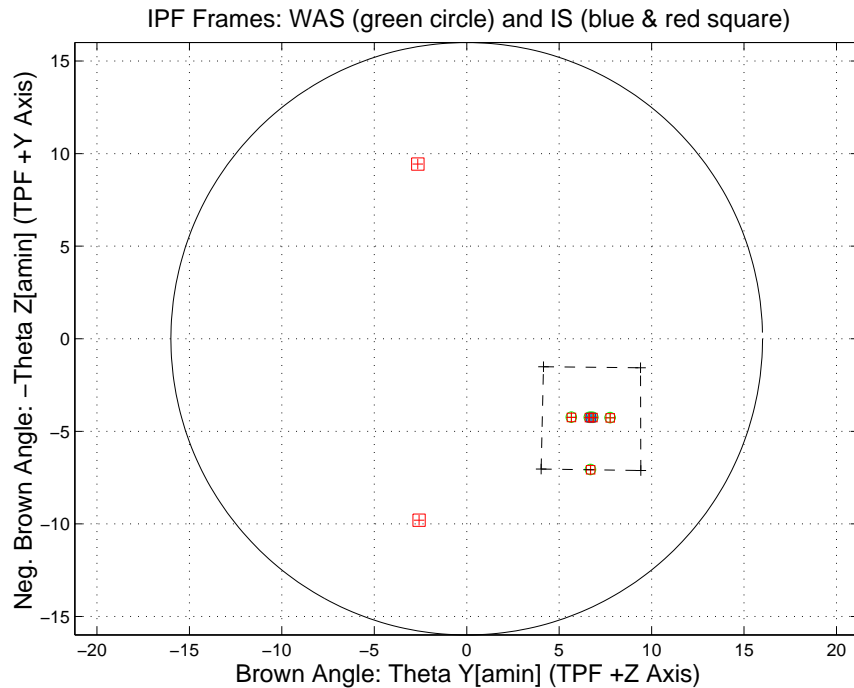


Figure 1.1: A-priori and a-posteriori IPF frames

RAW	FINAL (After Editing)
AA501095	AA501095
AS501095	AS501095
CA501095	CA502095
CB501095	CB501095
CS501095	CS501095

Table 1.1: IPF filter input files

EXECUTION CONFIGURATION ITEM	CURRENT STATUS
IPF Filter Version Used	IPF.V3.0.0B
Frame Table Version Used	BodyFrames_FTU_13a
Scan-Mirror Employed?	YES
IPF Filter Mode	NORMAL-MODE(0)
SLIT-MODE Operation	DISABLED
Kalman Filter Operation	ENABLED
Least-Squares Data Analysis	ENABLED
IBAD Screening	ENABLED
User-Specified Data Editing	DISABLED
Total Number of Iterations	25
LS Residual Sigma Scale	7.58215478E-001
Total Number of Maneuvers	7

Table 1.2: IPF filter execution configuration

Con. Plate Scale			Γ Dependent				Γ^2 Dependent				Linear Plate Scale						Mirror			
a_{00}	b_{00}	c_{00}	a_{10}	b_{10}	c_{10}	d_{10}	a_{20}	b_{20}	c_{20}	d_{20}	a_{01}	b_{01}	c_{01}	d_{01}	e_{01}	f_{01}	α	β		
1	2	3	4	5	6	7	8	9	10	11	12	13	14	15	16	17	18	19		
1	1	1	1	1	1	1	0	0	0	0	1	1	1	1	1	1	1	1		
IPF (T)			Alignment R						Gyro Drift Bias											
θ_1	θ_2	θ_3	a_{rx}	a_{ry}	a_{rz}	b_{rx}	b_{ry}	b_{rz}	c_{rx}	c_{ry}	c_{rz}	b_{gx}	b_{gy}	b_{gz}	c_{gx}	c_{gy}	c_{gz}			
20	21	22	23	24	25	26	27	28	29	30	31	32	33	34	35	36	37			
1	1	1	1	1	1	1	1	1	1	1	1	1	1	1	1	1	1			

Table 1.3: IPF filter execution mask vector assignment

FOCAL PLANE SURVEY ANALYSIS: IOC Fine Survey.

INSTRUMENT NAME: MIPS_24um_center NF: 95

PIX2RADW: 1.20874169E-005 [rad/pixel] = 2.4932E+000 [arcsec/pixel]

PIX2RADV: 1.25959084E-005 [rad/pixel] = 2.5981E+000 [arcsec/pixel]

FRAME	DESCRIPTION	IPF ¹	SF ²	TOTAL	REQ
095(P)	MIPS_24um_center	0.0298	0.0855	0.0906	0.14
096(I)	MIPS_24um_plusY_edge	0.0472	0.0855	0.0977	N/A
099(I)	MIPS_24um_small_FOV1	0.0279	0.0855	0.0899	N/A
100(I)	MIPS_24um_small_FOV2	0.0296	0.0855	0.0905	N/A
103(I)	MIPS_24um_large_FOV1	0.0297	0.0855	0.0905	N/A
104(I)	MIPS_24um_large_FOV2	0.0299	0.0855	0.0906	N/A

Table 1.4: IPF calibration error summary ([arcsec], 1-sigma, radial)

RMS METRIC	A PRIORI ³	A POSTERIORI ³	ATT. CORRECTED ⁴	UNITS
Radial	2.5097	0.1539	0.1444	arcsec
W-Axis	1.1533	0.1037	0.0909	arcsec
V-Axis	2.2290	0.1137	0.1122	arcsec
Radial	0.9747	0.0604	0.0565	pixels
W-Axis	0.4626	0.0416	0.0365	pixels
V-Axis	0.8579	0.0438	0.0432	pixels

Table 1.5: Science measurement prediction error summary (1-sigma)

¹IPF filter removes systematic pointing errors due to: thermomechanical alignment drift (Body to TPF), gyro bias and bias drift, centroiding error, attitude error, and optical distortion. IPF SIGMA presented here is “Scaled” by the Least Squares Scale factor. The Least Squares Scale Factor was: 0.758215. It is assumed that the gyro Angle Random Walk contribution is captured with the Least Squares scaling. The gyro ARW contribution can be approximately calculated as 0.0756 arcseconds, given that ARW = 100 $\mu\text{deg}/\sqrt{\text{hr}}$, with 5.562000e+002 second Maneuver time (max), and 7 independent Maneuvres.

²Gyro Scale Factor(GSF) assumes 95 ppm error over 0.250 degree maneuver.

³This can be interpreted as estimate of ”pixel to sky” pointing reconstruction error if no science data is used.

⁴This can be interpreted as estimate of achieved S/I centroiding error

IPF BROWN ANGLE SUMMARY					
FRAME TABLE USED: BodyFrames_FTU_13a					
NF	NAME	WAS	IS	CHANGE	UNIT
095	theta_Y	+6.716105	+6.722262	+0.006157	arcmin
095	theta_Z	+4.246060	+4.261820	+0.015760	arcmin
095	angle	+0.637930	+0.634863	-0.003066	deg
096	theta_Y	+6.695190	+6.704089	+0.008900	arcmin
096	theta_Z	+7.060913	+7.074454	+0.013541	arcmin
096	angle	+0.637930	+0.634863	-0.003066	deg
099	theta_Y	+7.756798	+7.763455	+0.006657	arcmin
099	theta_Z	+4.259313	+4.275316	+0.016003	arcmin
099	angle	+0.637930	+0.634863	-0.003066	deg
100	theta_Y	+5.659609	+5.665413	+0.005804	arcmin
100	theta_Z	+4.234140	+4.249600	+0.015460	arcmin
100	angle	+0.637930	+0.634863	-0.003066	deg
103	theta_Y	+6.819955	+6.826155	+0.006200	arcmin
103	theta_Z	+4.247316	+4.263102	+0.015786	arcmin
103	angle	+0.637930	+0.634863	-0.003066	deg
104	theta_Y	+6.633060	+6.639183	+0.006123	arcmin
104	theta_Z	+4.245067	+4.260805	+0.015738	arcmin
104	angle	+0.637930	+0.634863	-0.003066	deg

Table 1.6: IPF Brown angle summary

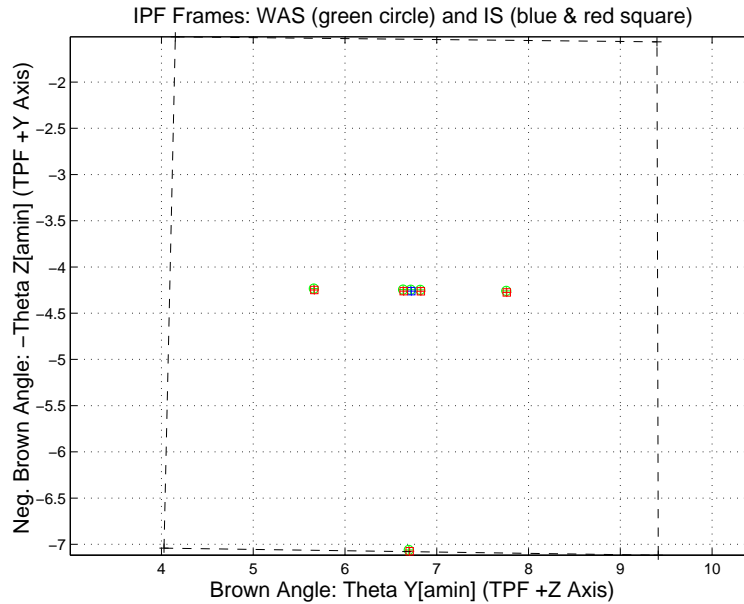


Figure 1.2: A-priori and a-posteriori IPF frames (ZOOMED)

2 IPF INPUT FILE HISTORY

STATUS	FILENAME	START TIME	END TIME
WAS	AA501095	752784500.5	752790000.4
IS	AA501095	752784500.5	752790000.4
WAS	CA501095	752785519.5	752789248.5
IS	CA502095	752785519.5	752789248.5
WAS	CB501095	752785324.7	752789394.8
IS	CB501095	752785324.7	752789394.8

Table 2.1: IPF input file begin and end times

WAS	SIZE	IS	SIZE	REMOVED	PATCHED
AA501095	55000	AA501095	55000	0	0
CA501095	218	CA502095	214	4	N/A
CB501095	63	CB501095	63	0	N/A

Table 2.2: IPF input file editing status

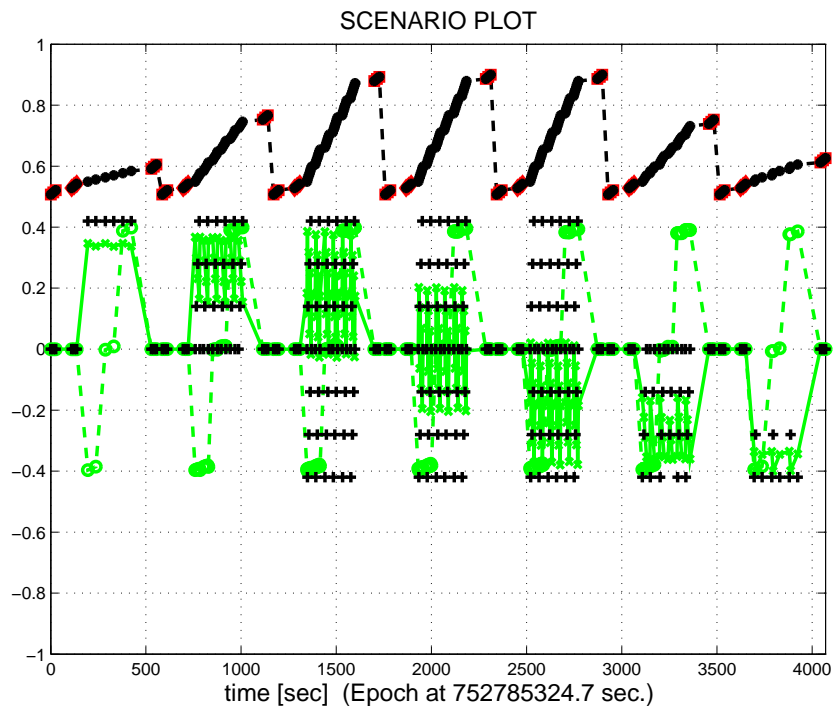


Figure 2.1: Scenario Plot

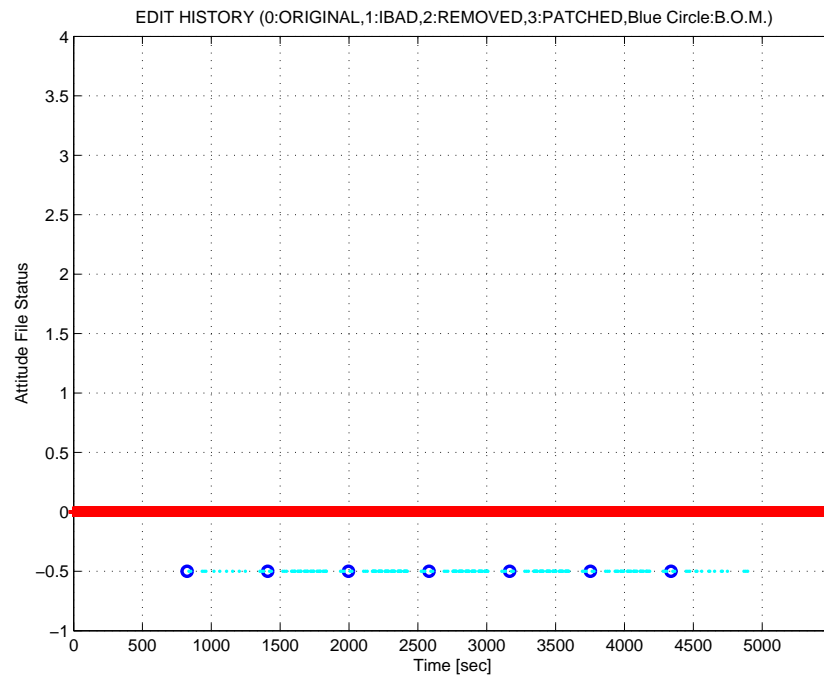


Figure 2.2: Attitude file edit history

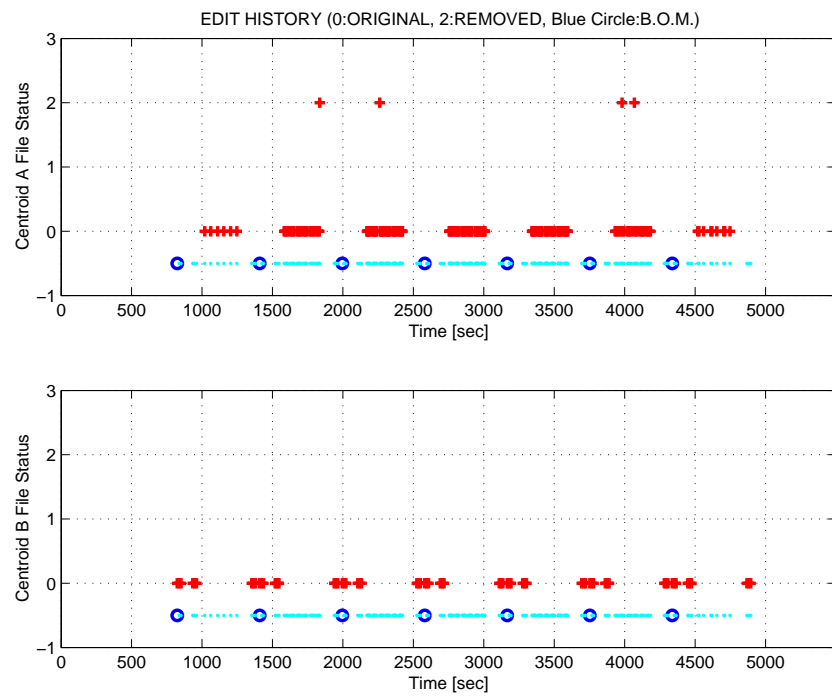


Figure 2.3: Centroid file edit history

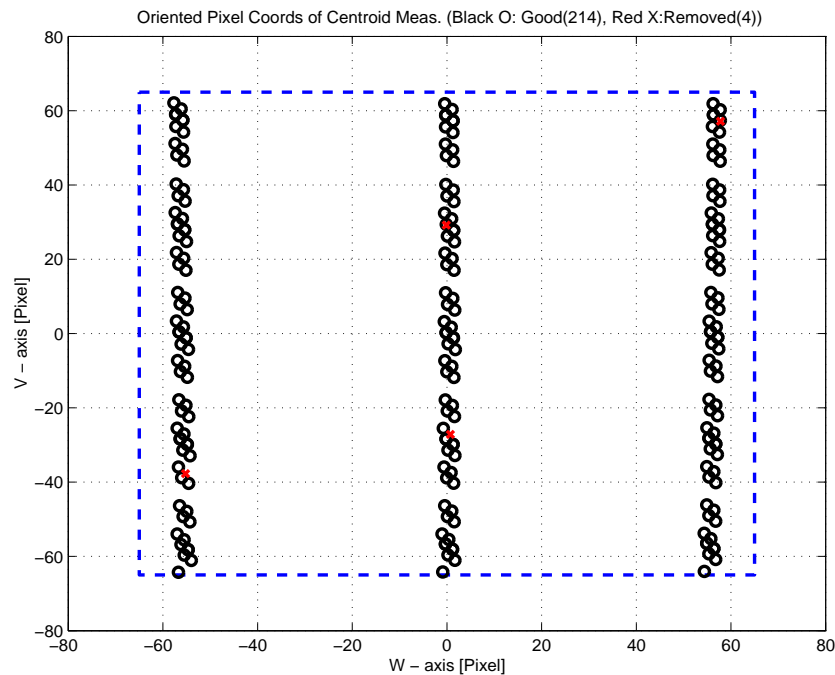


Figure 2.4: Oriented Pixel Coords of Centroid Meas. Edited Centroids

LIST OF REMOVED SCIENCE CENTROIDS									
36	53	187	196						

Table 2.3: List of Removed Centroids (Original CA File Row Index)

LIST OF REMOVED PCRS CENTROIDS									

Table 2.4: List of Removed PCRS Centroids (Original CB File Row Index)

3 IPF EXECUTION RESULTS

3.1 IPF EXECUTION OUTPUT PLOTS

This subsection summarizes the IPF filter results. As shown in Table 3.1, the output plots are segmented to three groups: predicted performance, post-run results and IPF trending plots.

FIGURE NO.	DESCRIPTION
Predicted performance prior to IPF run	
Figure 3.1	Meas. and a-priori predicts in TPF coords
Figure 3.2	Meas. and a-priori predicts in Oriented Pixel Coords including rectangular array boundary approximation
Figure 3.3	A-Priori Prediction Error Quiver Plot in Oriented Pixel Coords including rectangular array boundary approximation
Figure 3.4	A-priori prediction error
Figure 3.5	Oriented Pixel Coords of measurements and a-priori predicts (PCRS only)
Figure 3.6	Oriented Pixel Coords of measurements and a-priori predicts (Zoomed, PCRS only)
Figure 3.7	Oriented (W,V) Pixel Coords of A-Priori PCRS Prediction Error Quiver Plot
Figure 3.8	A-priori PCRS prediction error
IPF filter performance (post run results)	
Figure 3.9	IPF execution convergence, chart 1: (top) normalized residual error vs. iteration number and (bottom) norm of effective parameter corrections
Figure 3.10	IPF execution convergence, chart 2: parameter correction size vs. iteration number
Figure 3.11	Parameter uncertainty convergence: square-root of diagonal elements of covariance matrix vs. maneuver number
Figure 3.12	IPF parameter symbol table
Figure 3.13	KF parameter error sigma plot (a-priori-dashed, a-posteriori-solid). Includes true parameter errors (FLUTE runs only)
Figure 3.14	LS parameter error sigma plot. Includes true parameter errors (FLUTE runs only)
Figure 3.15	KF and LS parameter errors sigma plot (Figure 3.13 & Figure 3.14 combined)
Figure 3.16	Measurements and a-posteriori predicts in Oriented Pixel Coords including rectangular array boundaries (a-priori-dashed, a-posteriori-solid)
Figure 3.17	Attitude corrected meas. and a-posteriori predicts in Oriented Pixel Coords including rectangular array boundaries (a-priori-dashed, a-posteriori-solid)

Table 3.1: Table of figures I (IPF run)

FIGURE NO.	DESCRIPTION
IPF filter performance (post run results) - CONTINUE	
Figure 3.18	KF innovations with (o) and w/o (+) attitude corrections
Figure 3.19	Histograms of science a-posteriori residuals (or innovations)
Figure 3.20	A-Posteriori Science Centroid Prediction Error Quiver (Att. Cor.)
Figure 3.21	Normalized A-Posteriori Science Centroid Prediction Errors
Figure 3.22	KF innovations with (o) and w/o (+) attitude corrections (PCRS)
Figure 3.23	Histograms of PCRS a-posteriori residuals (or innovations)
Figure 3.24	A-posteriori PCRS Prediction Summary
Figure 3.25	A-posteriori PCRS Prediction (PCRS 1 Only)
Figure 3.26	A-posteriori PCRS Prediction (PCRS 2 Only)
Figure 3.27	A-Posteriori PCRS Prediction Errors Quiver (Att. Cor.)
Figure 3.28	Normalized A-Posteriori PCRS Prediction Errors
Figure 3.29	W-axis KF innovations and 1-sigma bound
Figure 3.30	V-axis KF innovations and 1-sigma bound
Figure 3.31	Array plot with (solid) and w/o (dashed) optical distortion corrections
Figure 3.32	Optical Distortion Plot: total (x5 magnification)
Figure 3.33	Optical Distortion Plot: constant plate scales (x5 magnification)
Figure 3.34	Optical Distortion Plot: linear plate scale (x5 magnification)
Figure 3.35	Optical Distortion Plot: gamma terms (x5 magnification)
Figure 3.36	Scan Mirror Chops
Figure 3.37	IPF Frame Reconstruction
Figure 3.38	Center Pixel Reconstruction
IPF parameter trending plots	
Figure 3.39	Estimated attitude corrections (Body frame)
Figure 3.40	Estimated attitude error sigma plot (Body frame)
Figure 3.41	Systematic error attributed to thermo-mechanical boresight drift (equiv. angle in (W,V) coords)
Figure 3.42	Systematic error attributed to thermo-mechanical boresight drift (equiv. angle in Body frame)
Figure 3.43	Systematic error attributed to gyro drift bias (equiv. rate in (W,V) coords)
Figure 3.44	Systematic error attributed to gyro drift bias (equiv. angle in (W,V) coords)
Figure 3.45	Systematic error attributed to gyro drift bias (equiv. angle in Body frame)

Table 3.2: Table of figures II (IPF run)

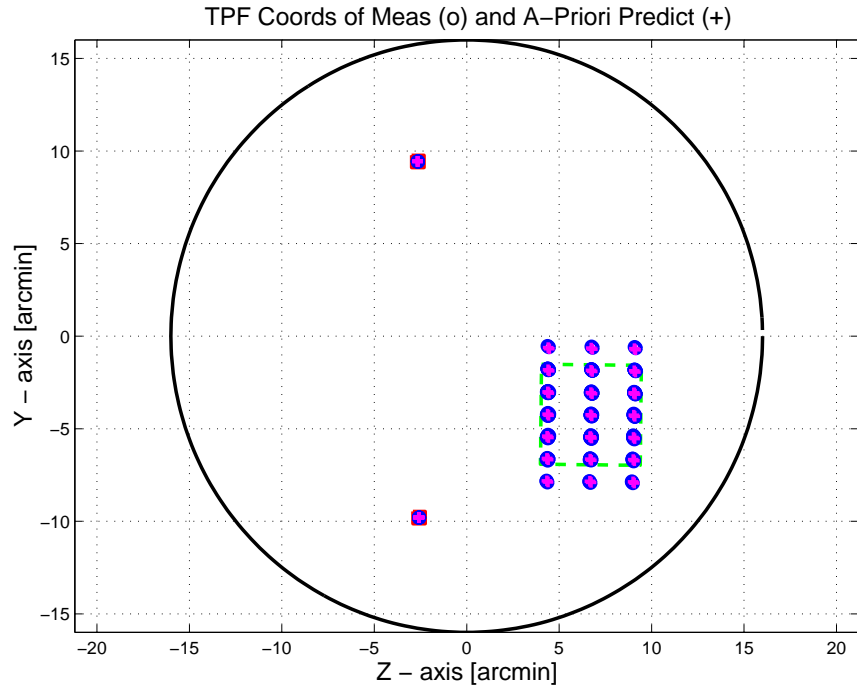


Figure 3.1: TPF coords of measurements and a-priori predicts

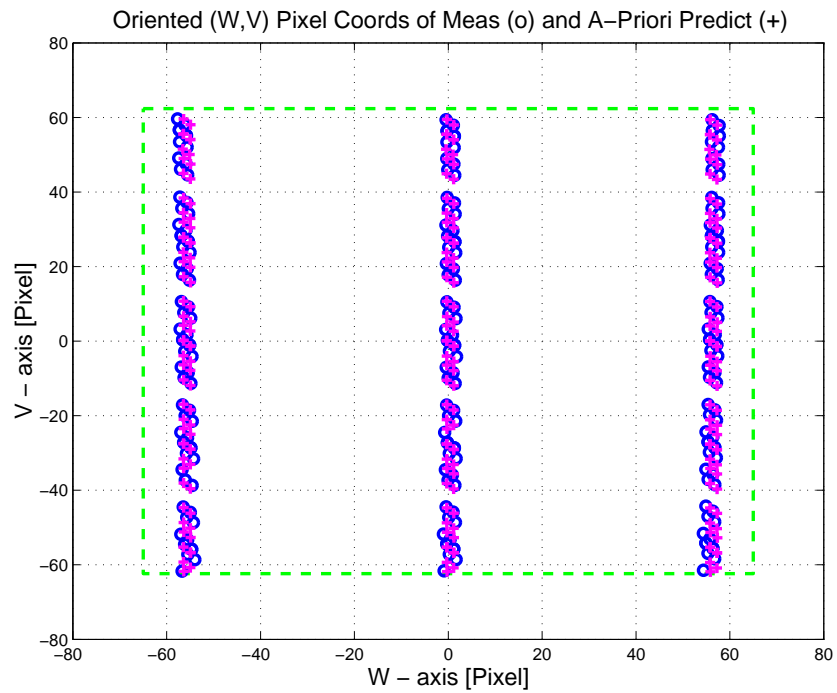


Figure 3.2: Oriented PixelCoords of measurements and a-priori predicts

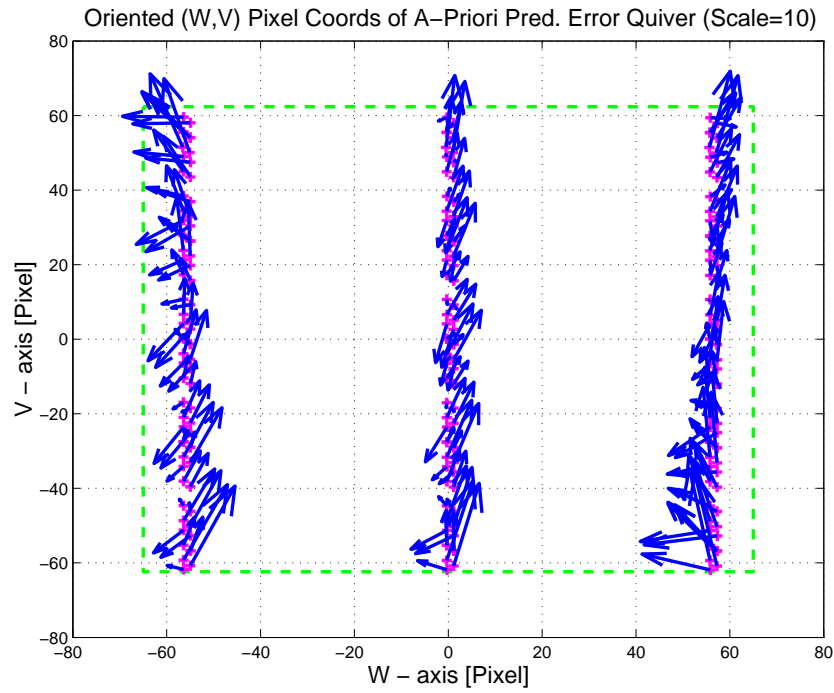


Figure 3.3: Oriented (W,V) Pixel Coords of A-Priori Prediction Error Quiver Plot

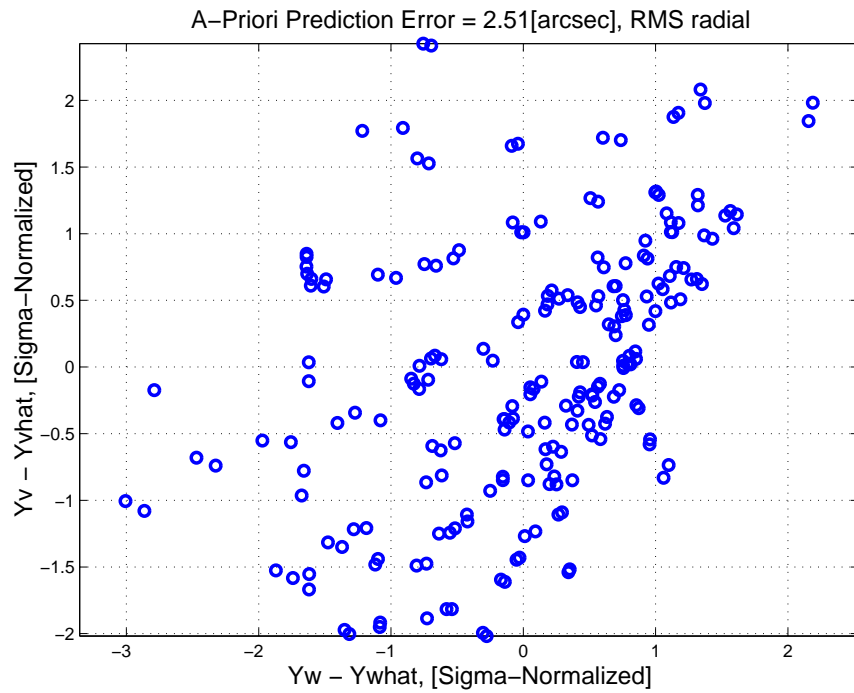


Figure 3.4: A-priori prediction error (Science Centroids)

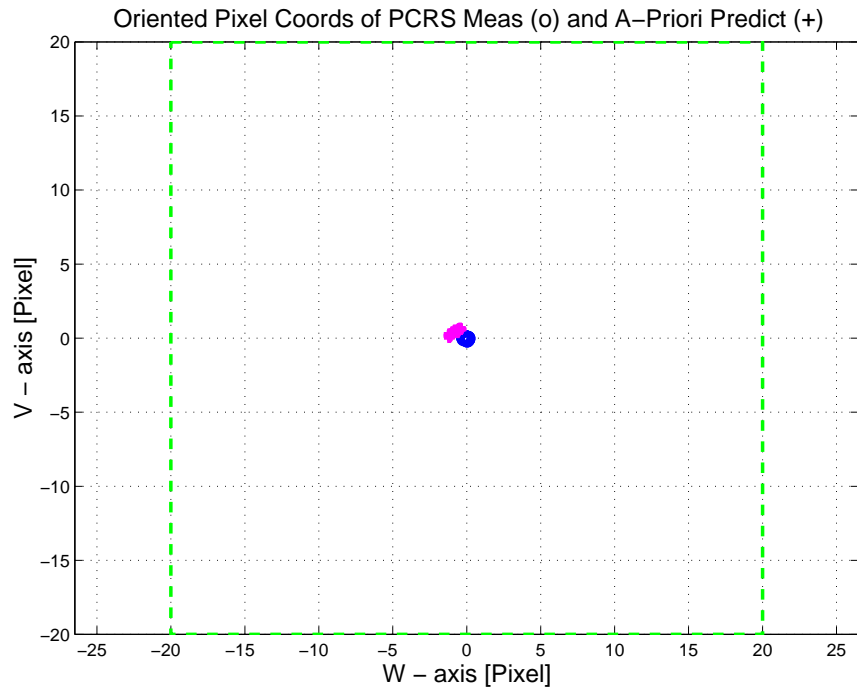


Figure 3.5: Oriented Pixel Coords of measurements and a-priori predicts (PCRS only)

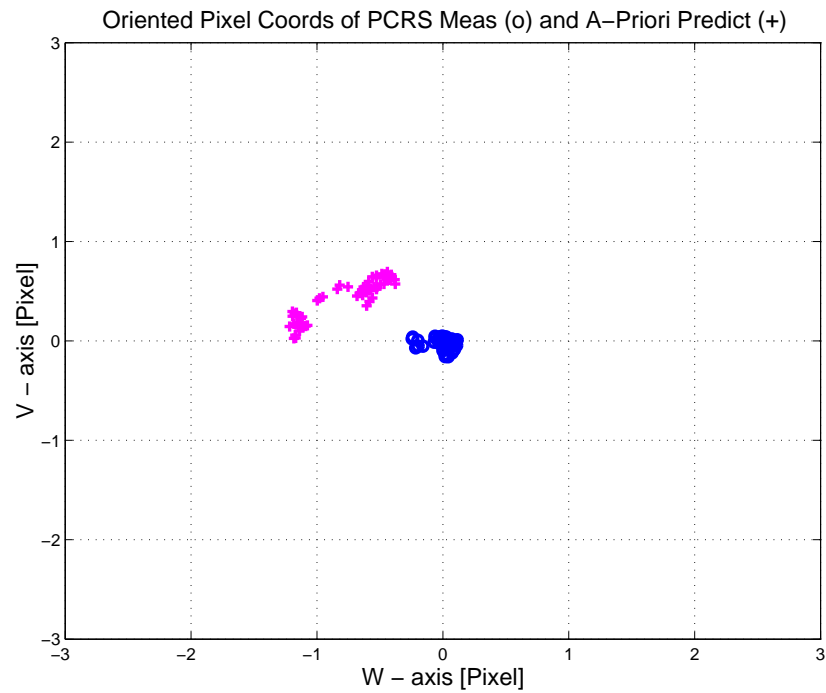


Figure 3.6: Oriented Pixel Coords of measurements and a-priori predicts (Zoomed, PCRS only)

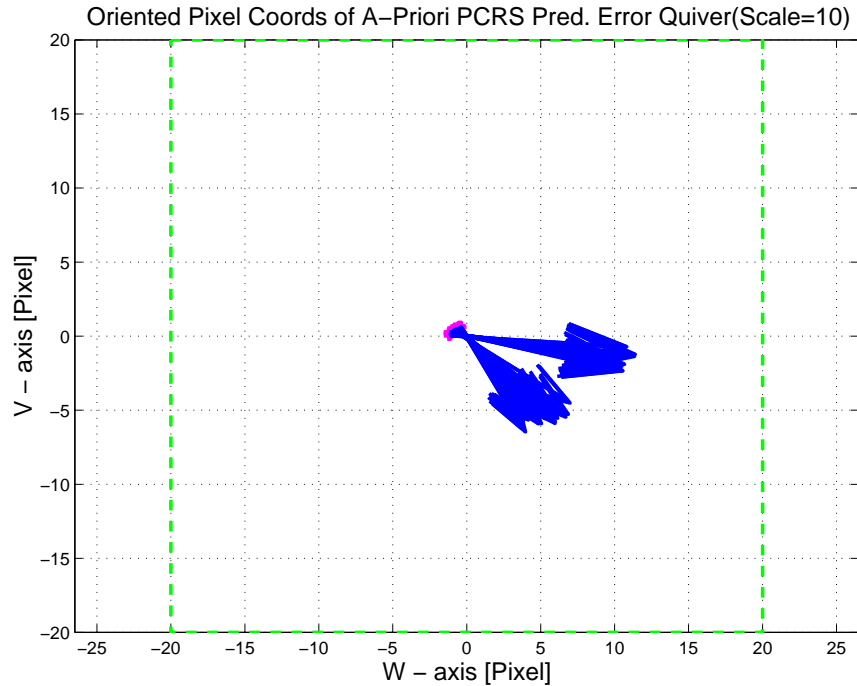


Figure 3.7: Oriented (W,V) Pixel Coords of A-Priori PCRS Prediction Error Quiver Plot

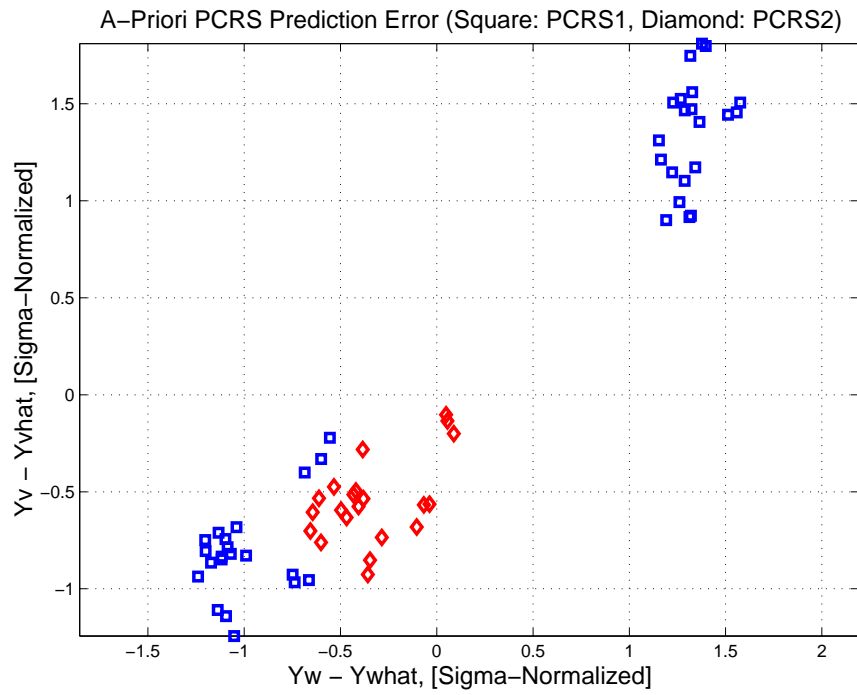


Figure 3.8: A-priori PCRS prediction error

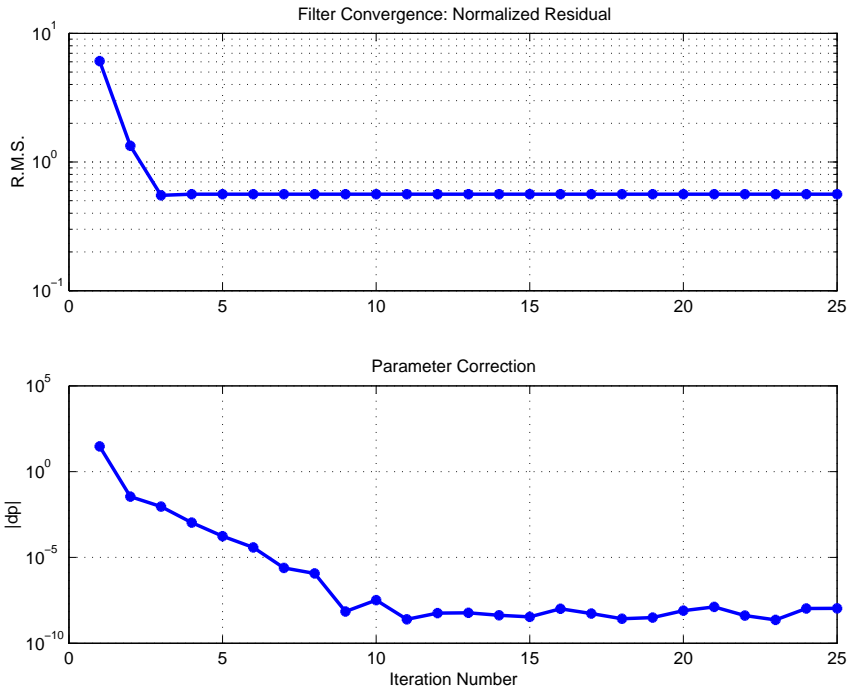


Figure 3.9: IPF execution convergence, chart 1

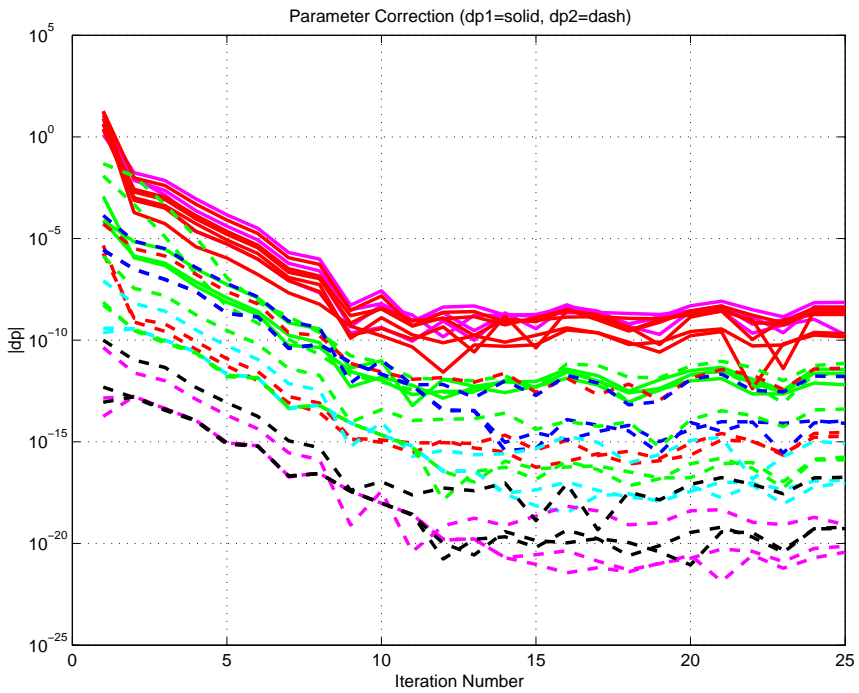


Figure 3.10: IPF execution convergence, chart 2

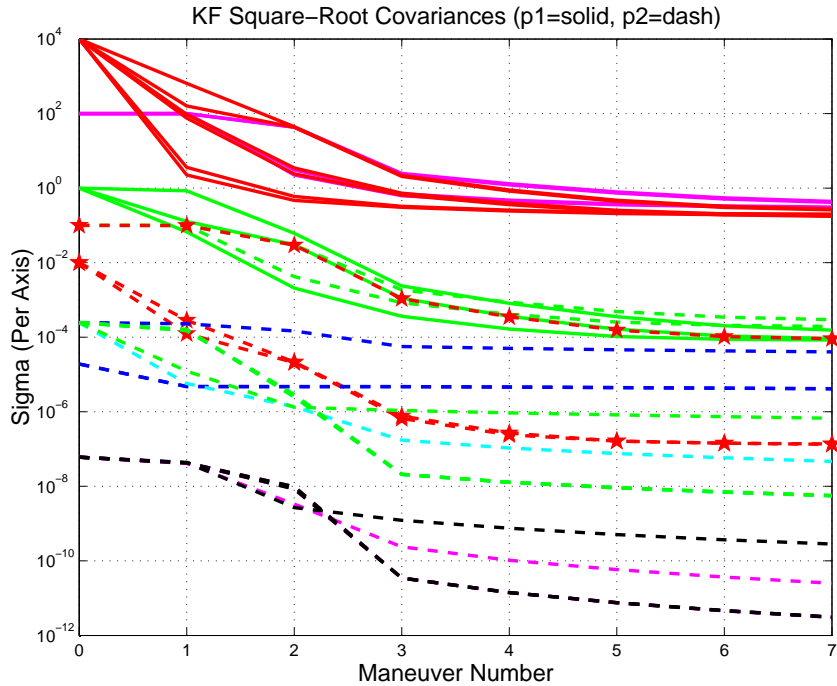


Figure 3.11: Parameter uncertainty convergence

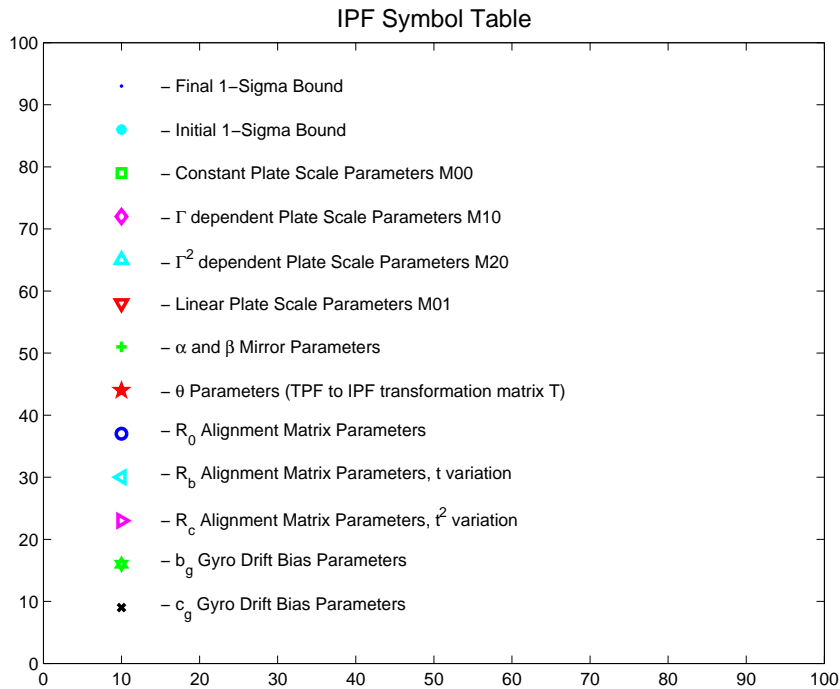


Figure 3.12: IPF parameter symbol table

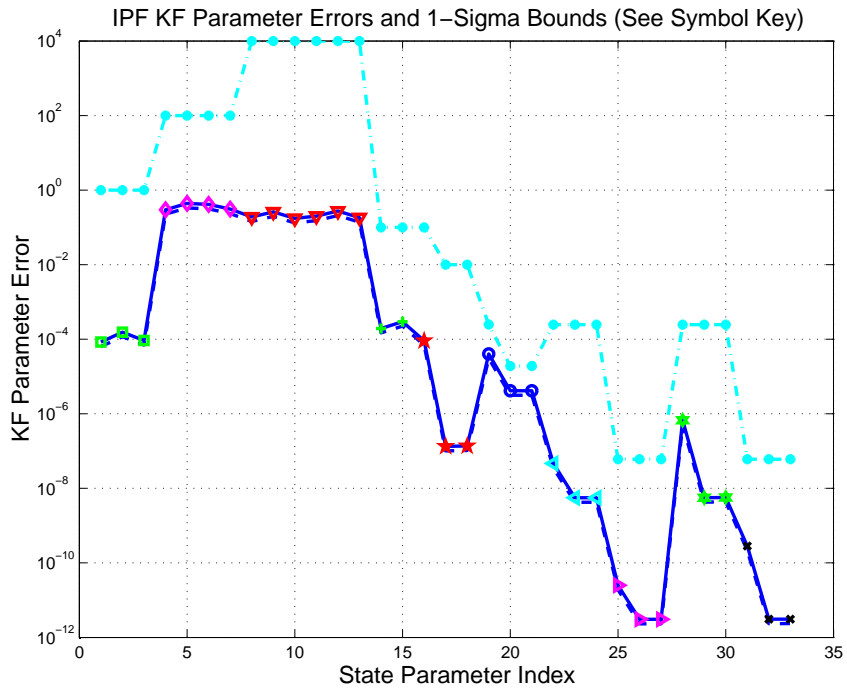


Figure 3.13: KF parameter error sigma plots

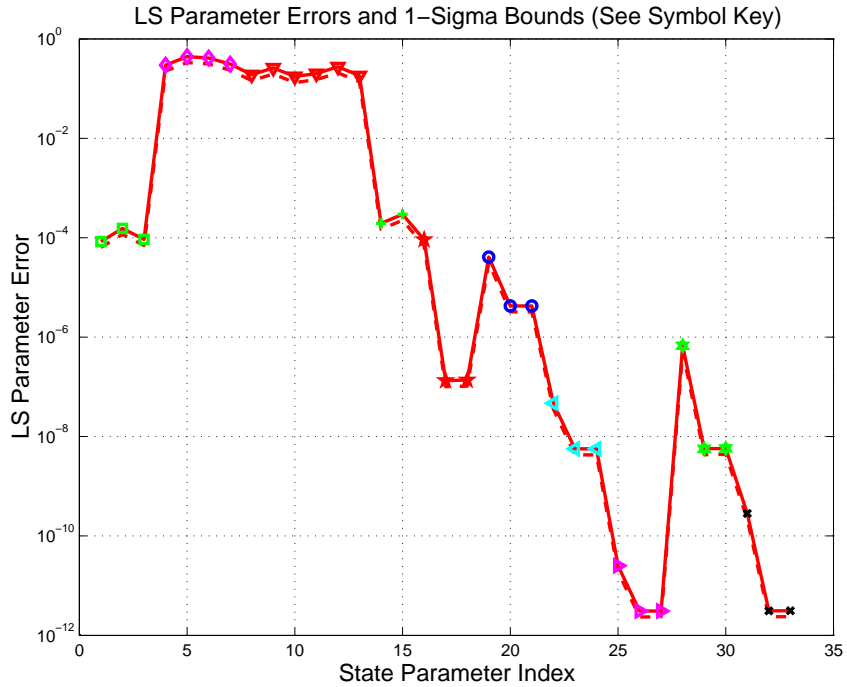


Figure 3.14: LS parameter error sigma plot

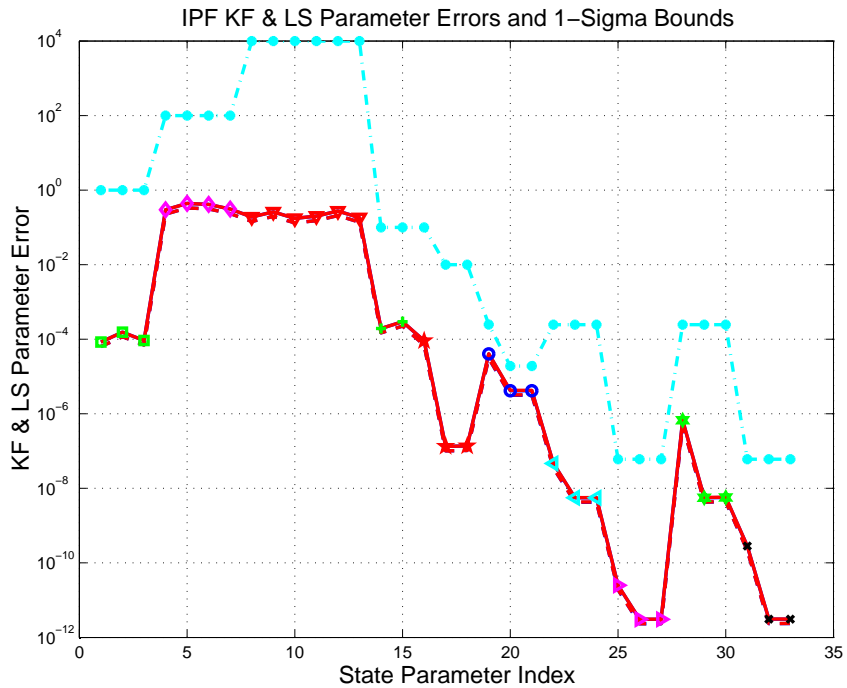


Figure 3.15: KF and LS parameter error sigma plot

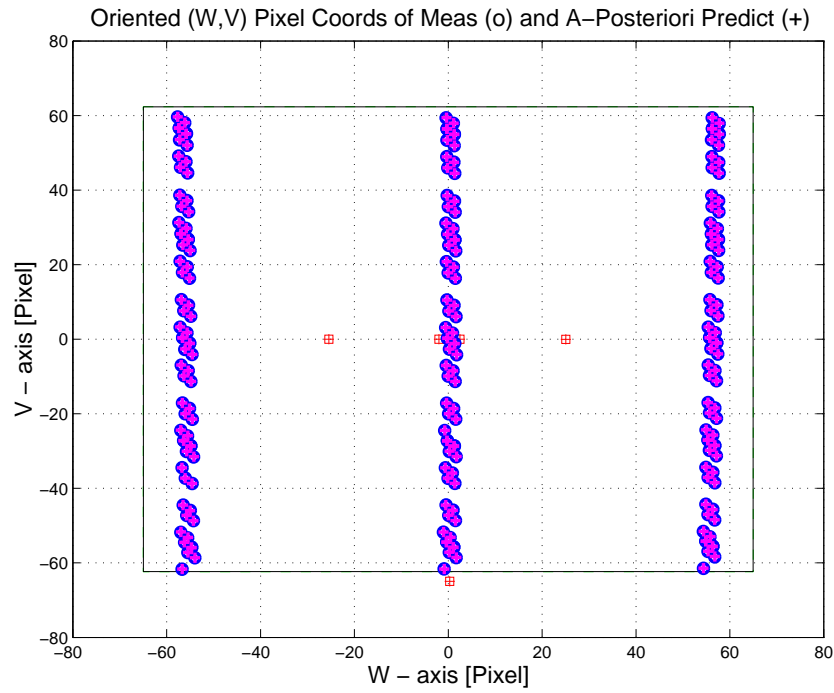


Figure 3.16: Oriented Pixel Coords of meas. and a-posteriori predicts

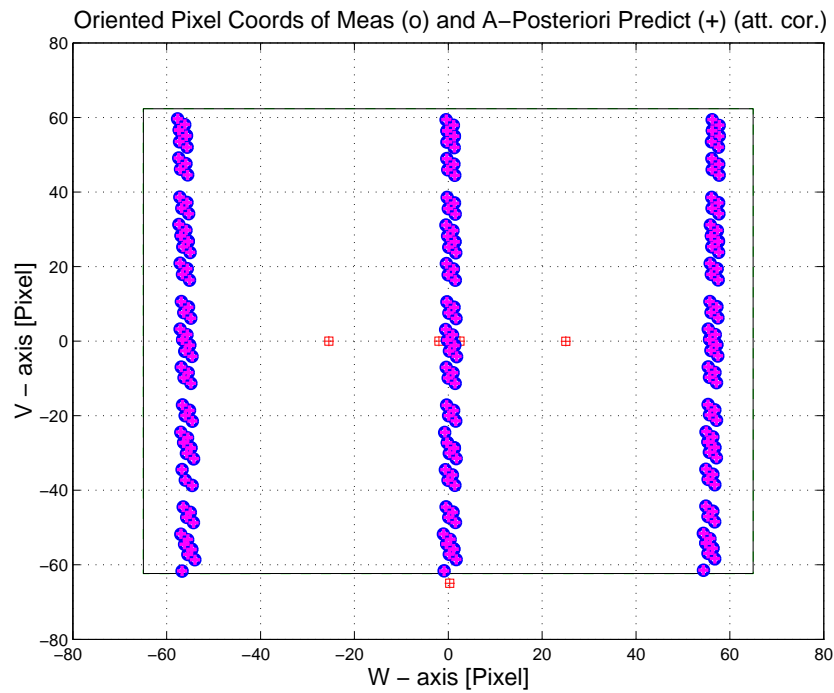


Figure 3.17: Oriented Pixel Coords of meas. and a-posteriori predicts (attitude corrected)

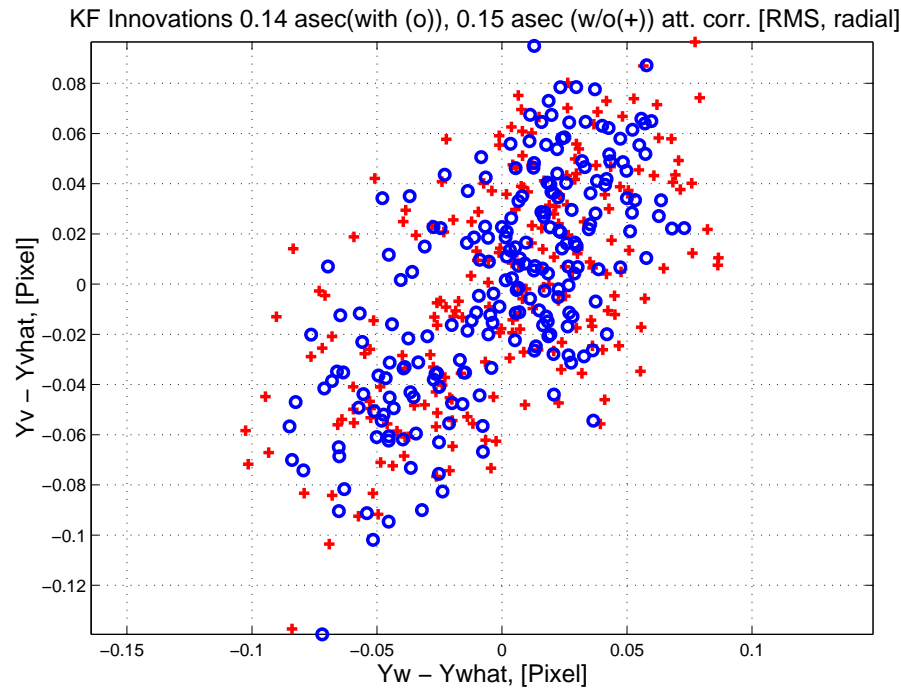


Figure 3.18: KF innovations with (o) and w/o (+) attitude corrections

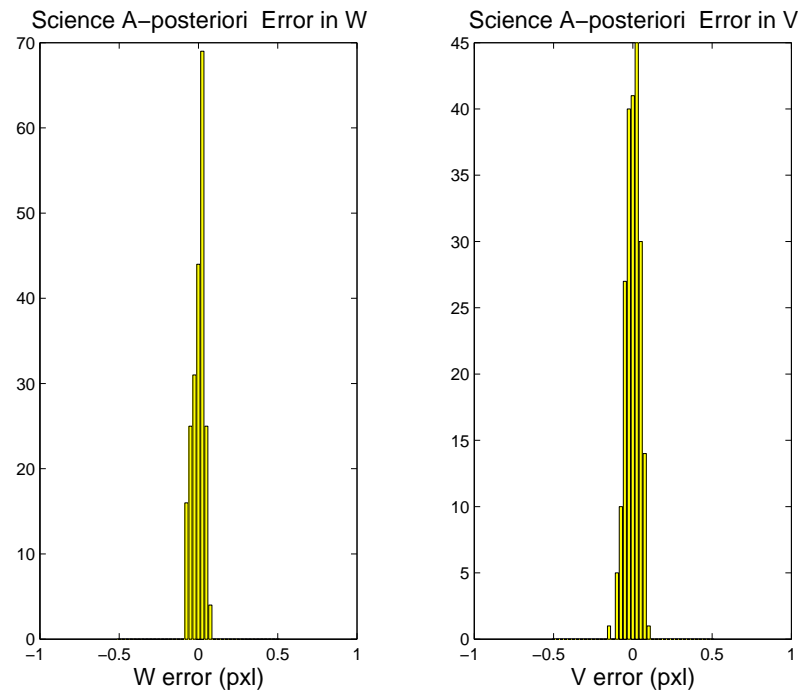


Figure 3.19: Histograms of science a-posteriori residuals (or innovations)

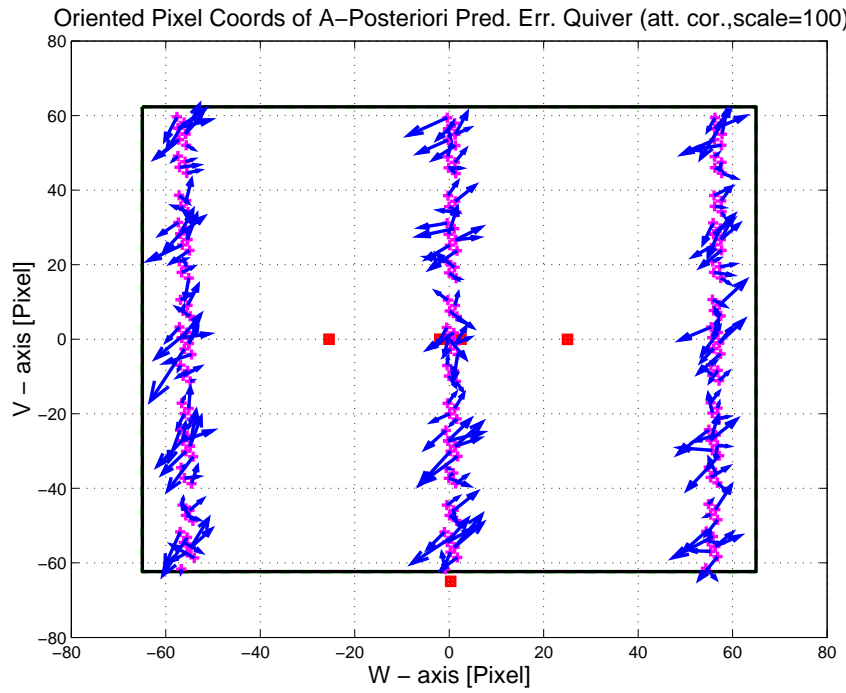


Figure 3.20: A-Posteriori Science Centroid Prediction Error Quiver (Att. Cor.)

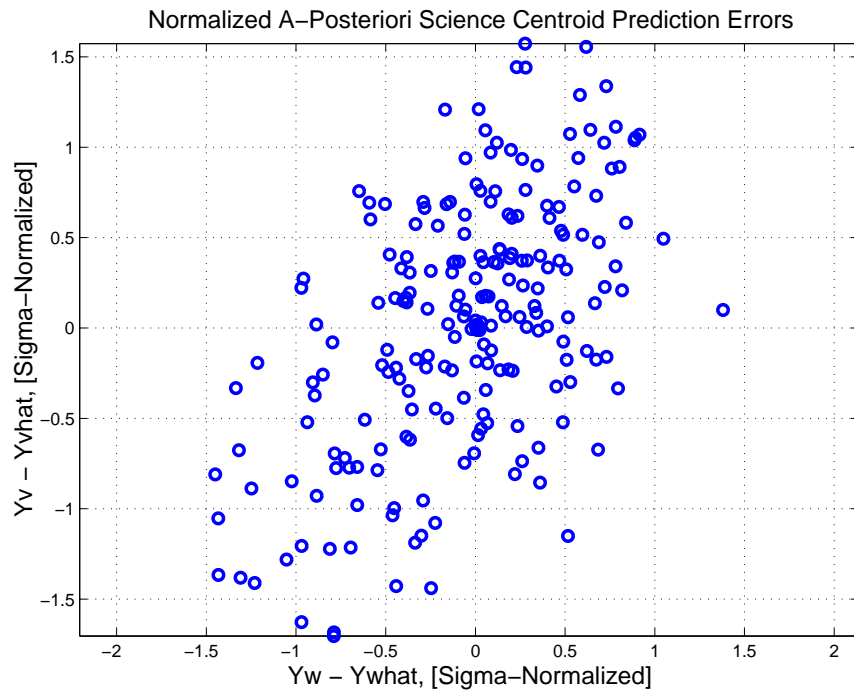


Figure 3.21: Normalized A-Posteriori Science Centroid Prediction Errors

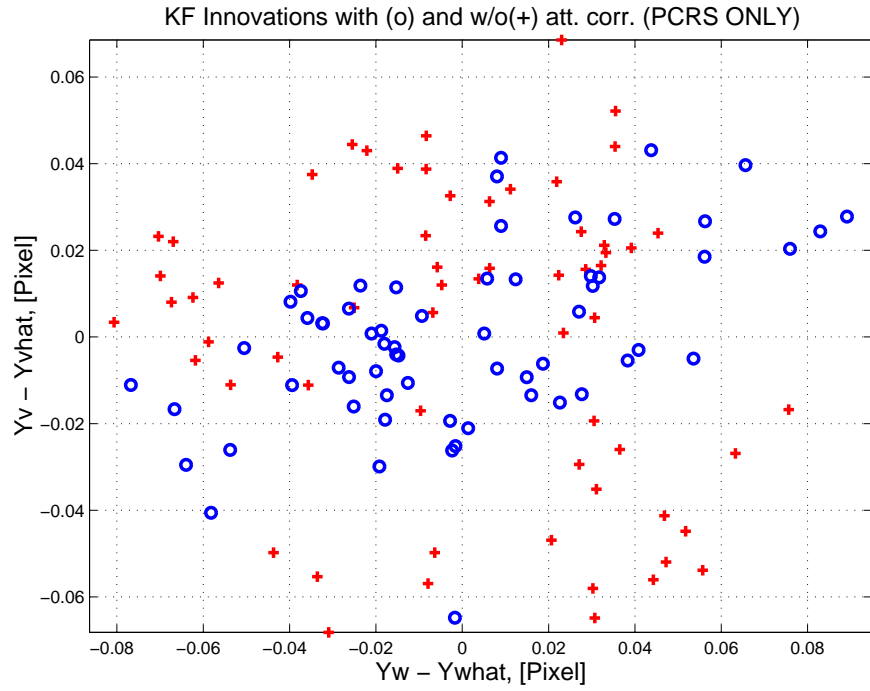


Figure 3.22: KF innovations with (o) and w/o (+) attitude corrections (PCRS)

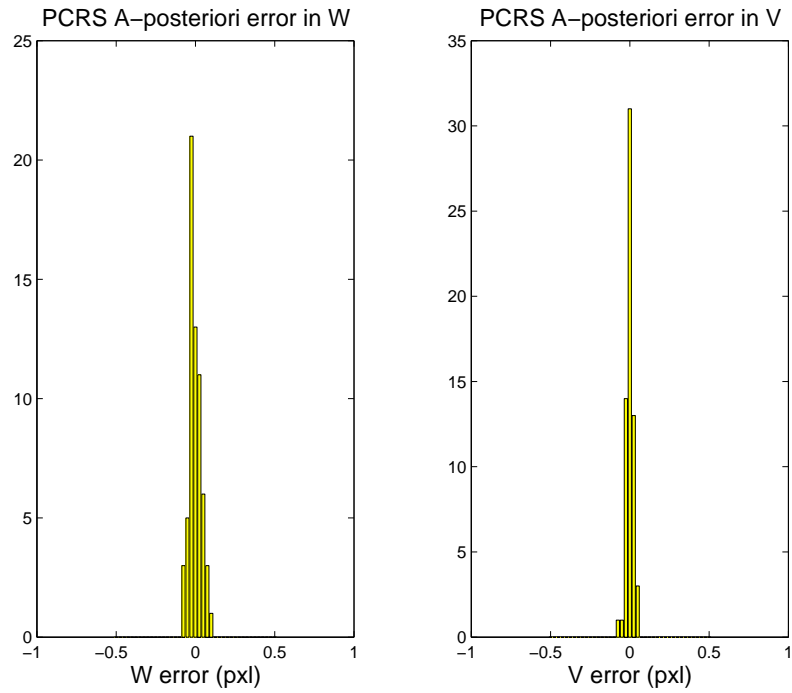


Figure 3.23: Histograms of PCRS a-posteriori residuals (or innovations)

IPF PCRS SUMMARY						
PCRS 1 (Total of 42 centroids)						
RMS	MEAN		SIGMA			
METRIC	APOST.	ATT. COR.	APOST.	ATT. COR.	STAT. CONF.	UNITS
Radial	0.0002	0.0002	0.0529	0.0475	0.0073	arcsec
W-axis	-0.0002	0.0000	0.0383	0.0414	0.0064	arcsec
V-axis	-0.0001	-0.0002	0.0365	0.0234	0.0036	arcsec
PCRS 2 (Total of 21 centroids)						
METRIC	APOST.	ATT. COR.	APOST.	ATT. COR.	STAT. CONF.	UNITS
Radial	0.0005	0.0004	0.0503	0.0281	0.0061	arcsec
W-axis	-0.0003	-0.0000	0.0411	0.0254	0.0055	arcsec
V-axis	0.0004	0.0004	0.0289	0.0119	0.0026	arcsec
Combined (Total of 63 centroids)						
METRIC	APOST.	ATT. COR.	APOST.	ATT. COR.	STAT. CONF.	UNITS
Radial	0.0002	0.0000	0.0520	0.0421	0.0053	arcsec
W-axis	-0.0002	0.0000	0.0393	0.0368	0.0046	arcsec
V-axis	0.0001	0.0000	0.0341	0.0203	0.0026	arcsec

Table 3.3: PCRS measurement prediction error summary

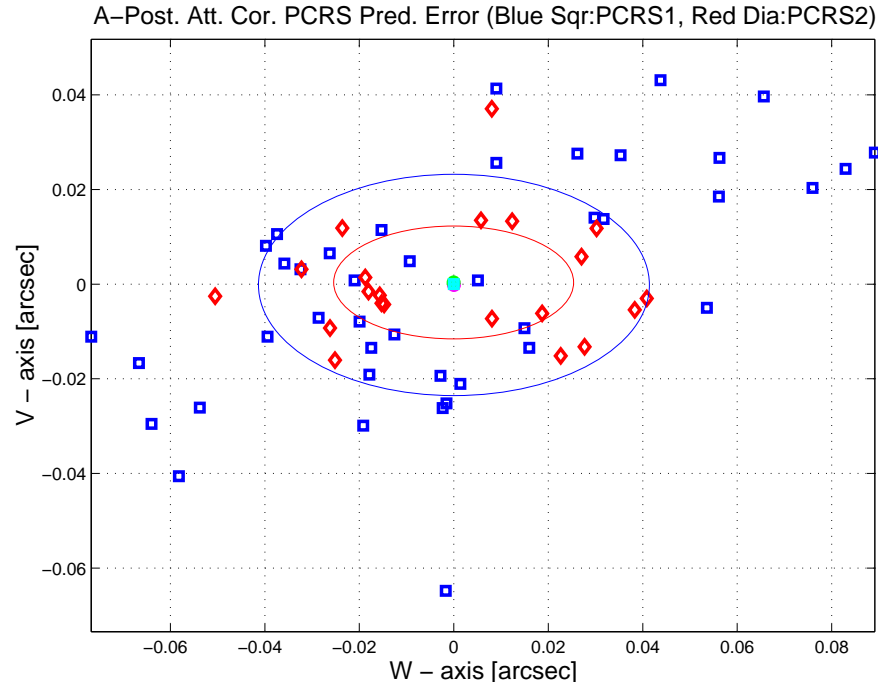


Figure 3.24: A-posteriori PCRS Prediction Summary

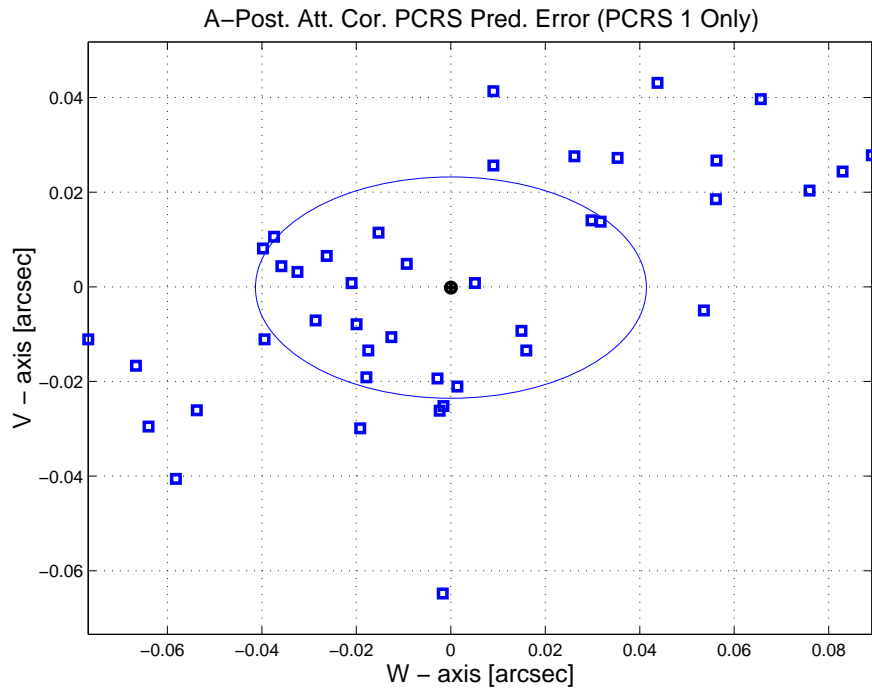


Figure 3.25: A-posteriori PCRS Prediction (PCRS 1 Only)

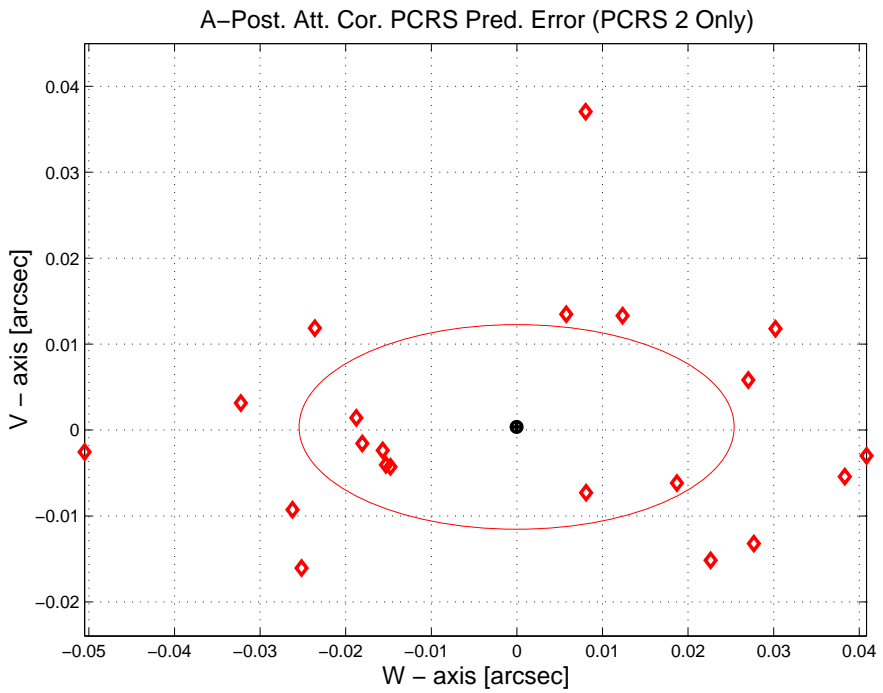


Figure 3.26: A-posteriori PCRS Prediction (PCRS 2 Only)

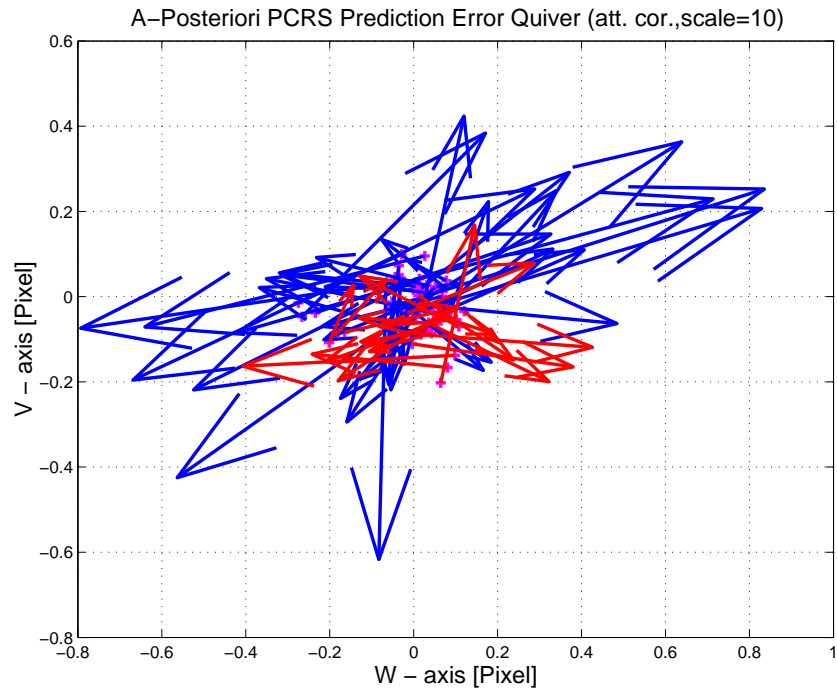


Figure 3.27: A–Posteriori PCRS Prediction Errors Quiver (Att. Cor.)

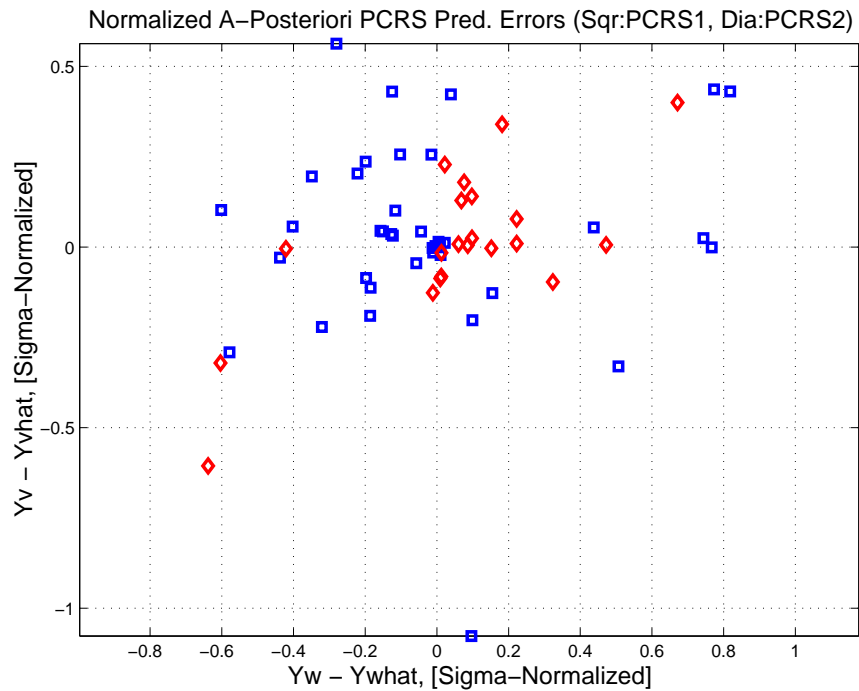


Figure 3.28: Normalized A–Posteriori PCRS Prediction Errors

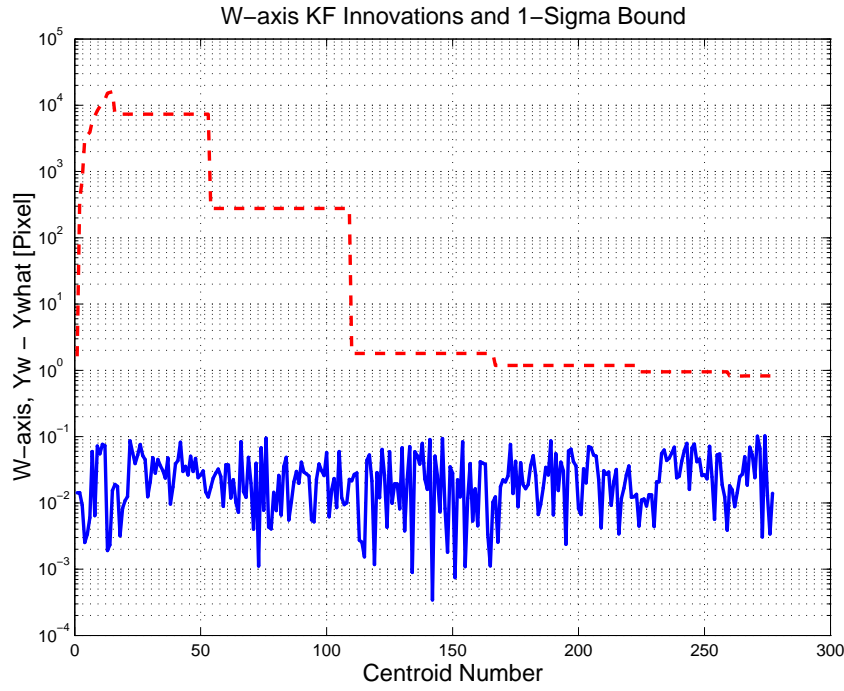


Figure 3.29: W-axis KF innovations and 1-sigma bound

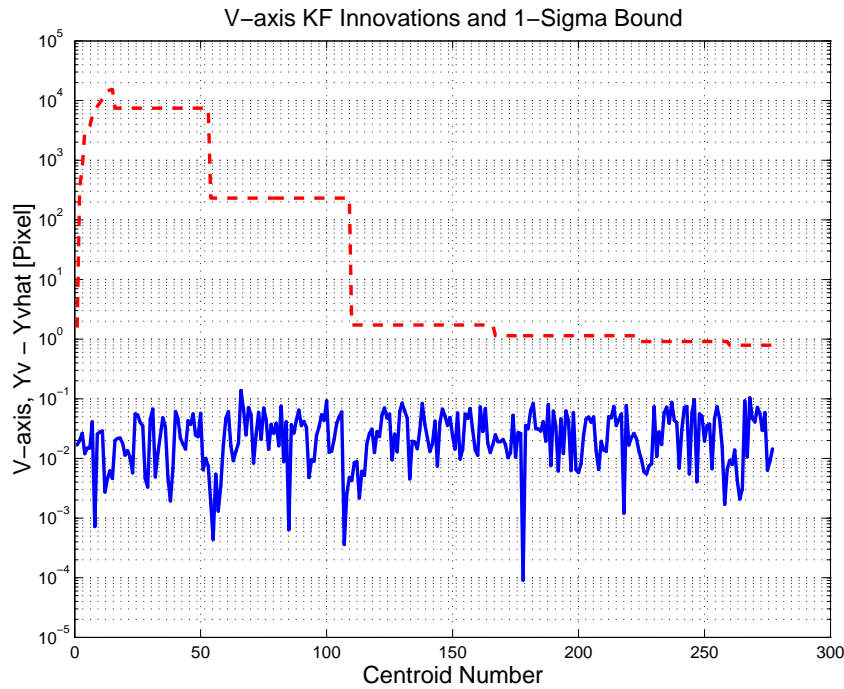


Figure 3.30: V-axis KF innovations and 1-sigma bound

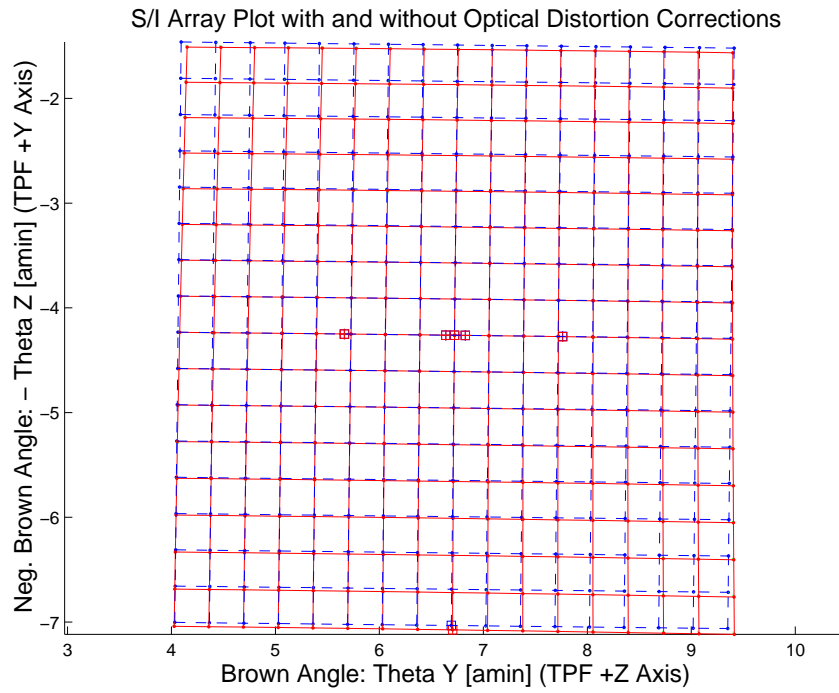


Figure 3.31: Array plot with (solid) and w/o (dashed) optical distortion corrections

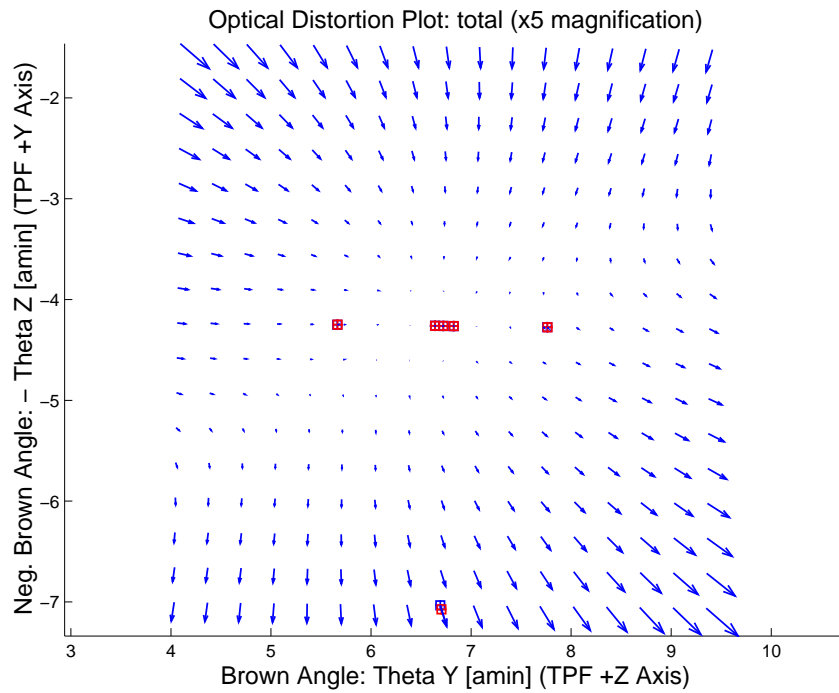


Figure 3.32: Optical Distortion Plot: total (x5 magnification)

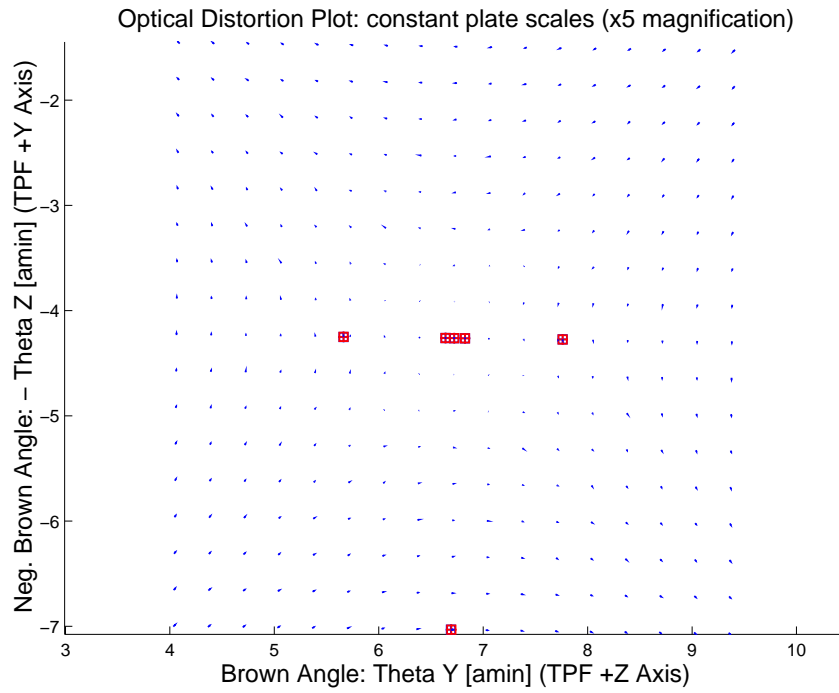


Figure 3.33: Optical Distortion Plot: constant plate scales (x5 magnification)

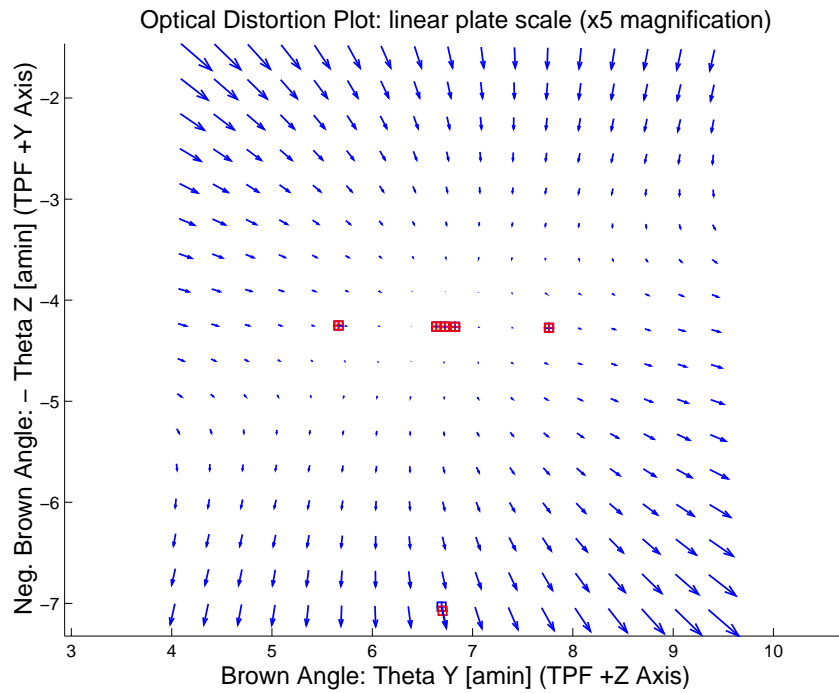


Figure 3.34: Optical Distortion Plot: linear plate scale (x5 magnification)

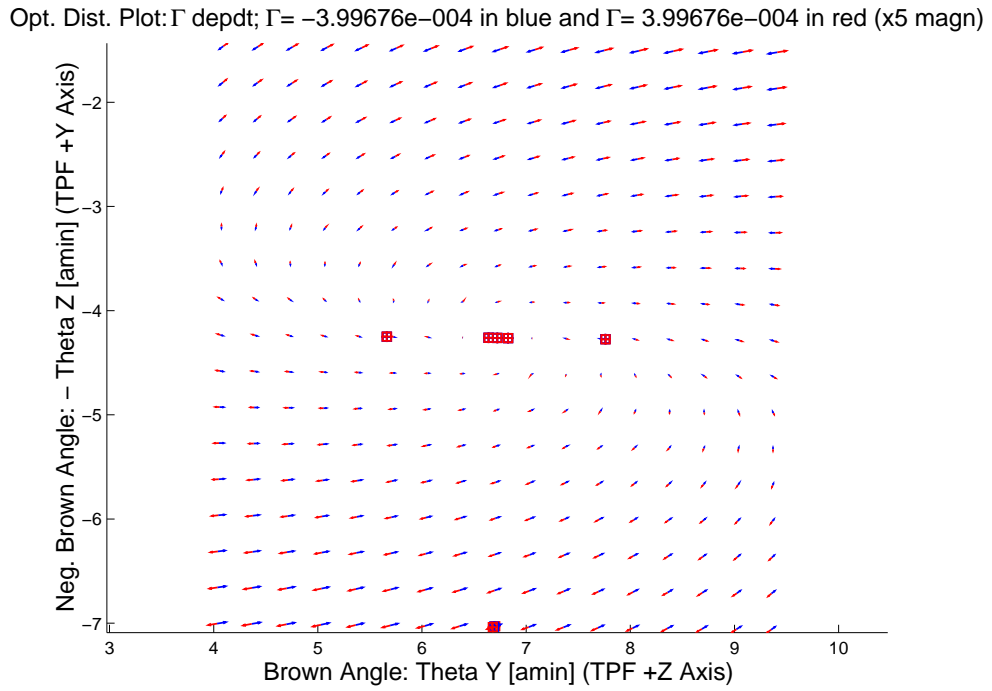


Figure 3.35: Optical Distortion Plot: gamma terms (x5 magnification)

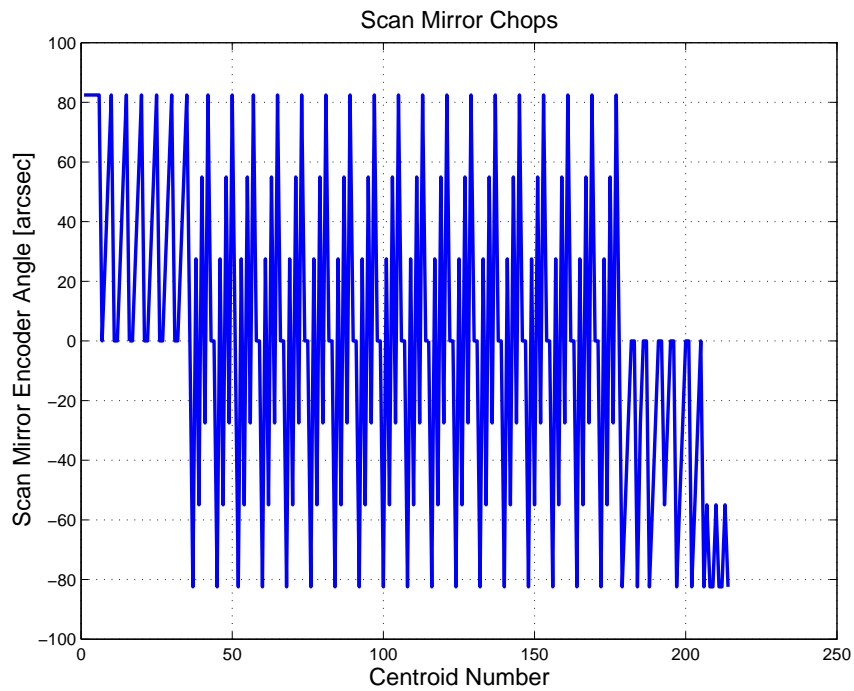


Figure 3.36: Scan Mirror Chops

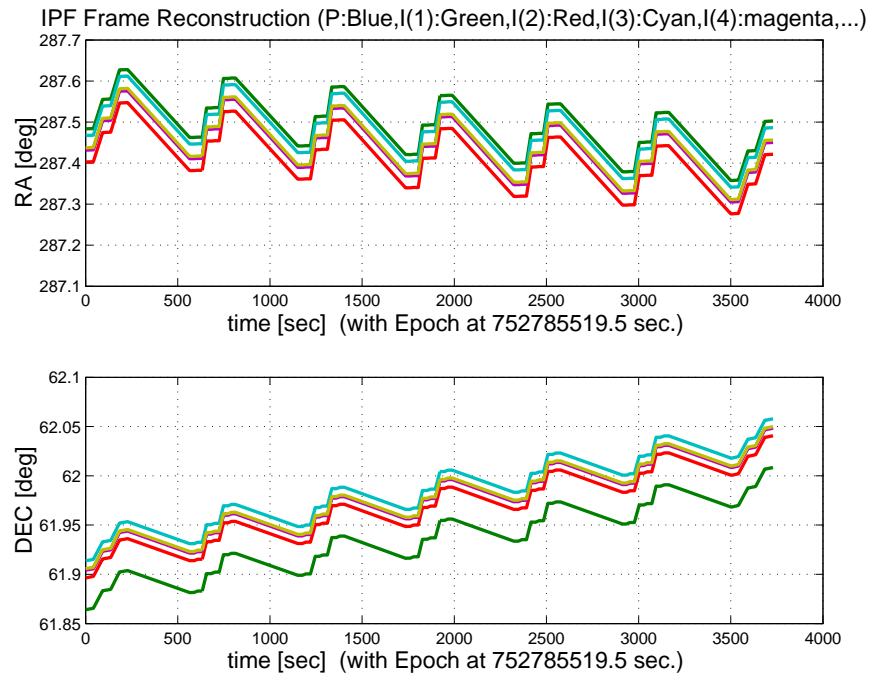


Figure 3.37: IPF Frame Reconstruction

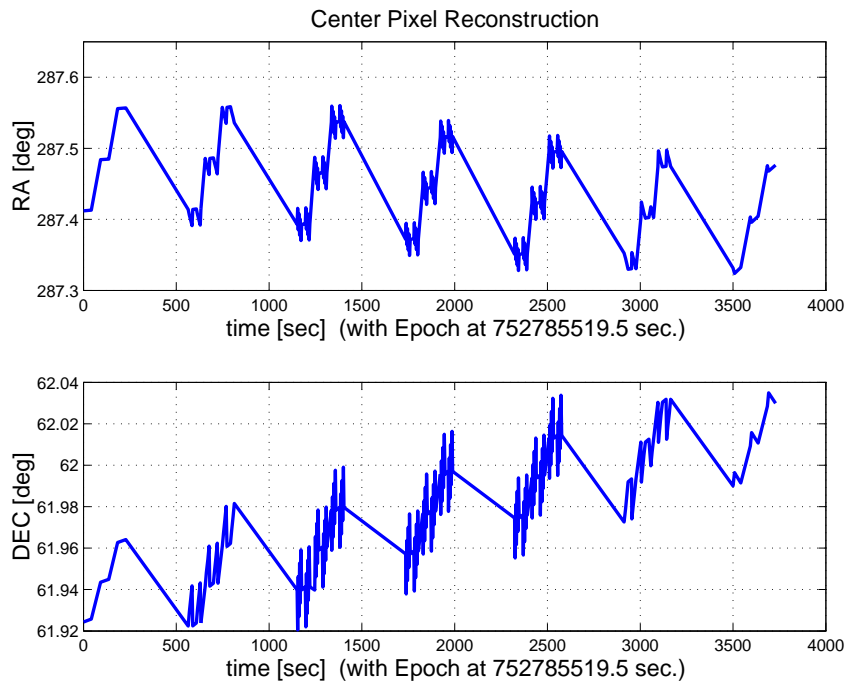


Figure 3.38: Center Pixel Reconstruction

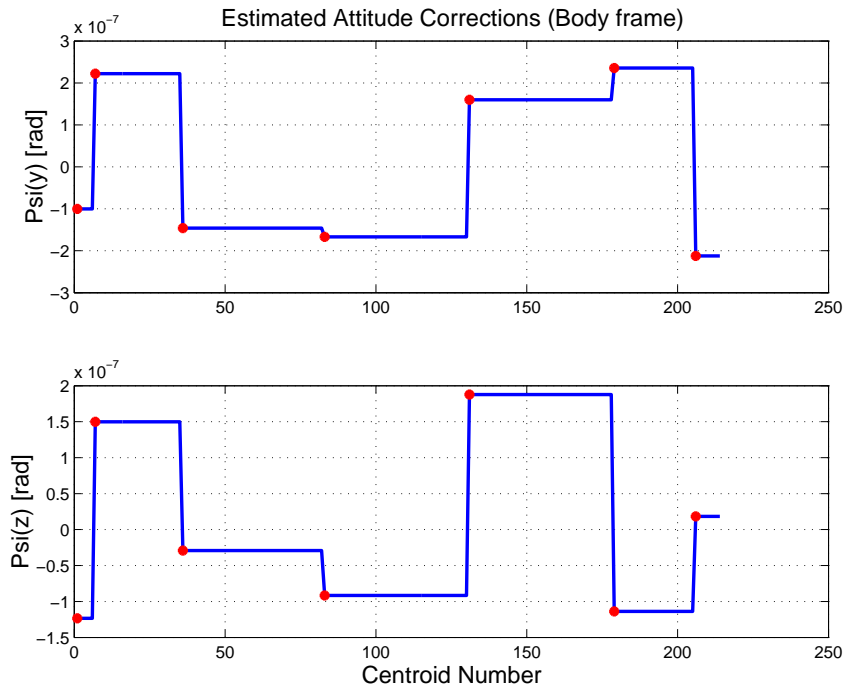


Figure 3.39: Estimated attitude corrections (Body frame)

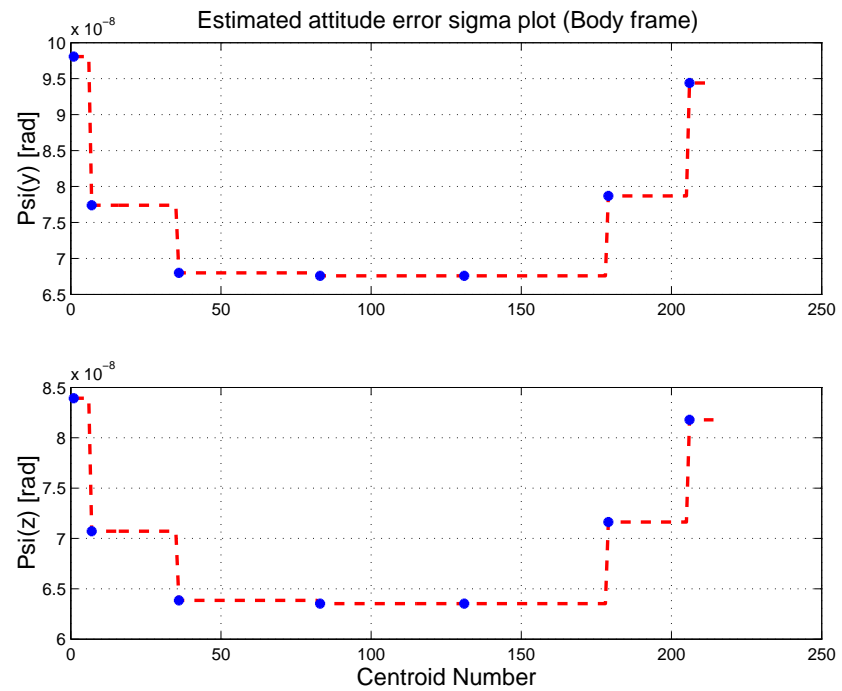


Figure 3.40: Estimated attitude error sigma plot (Body frame)

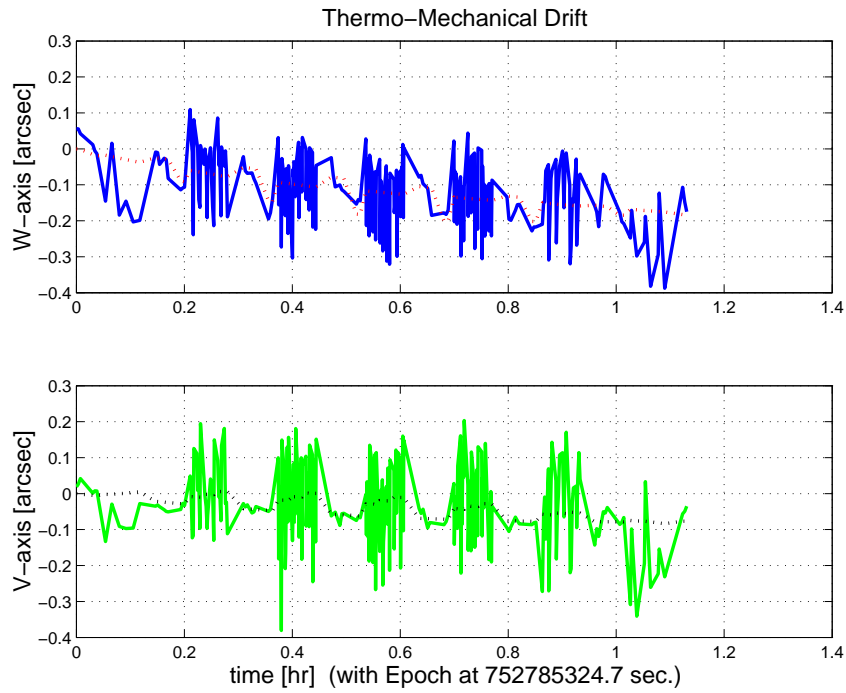


Figure 3.41: Thermo-mechanical boresight drift (equiv. angle in (W,V) coords)

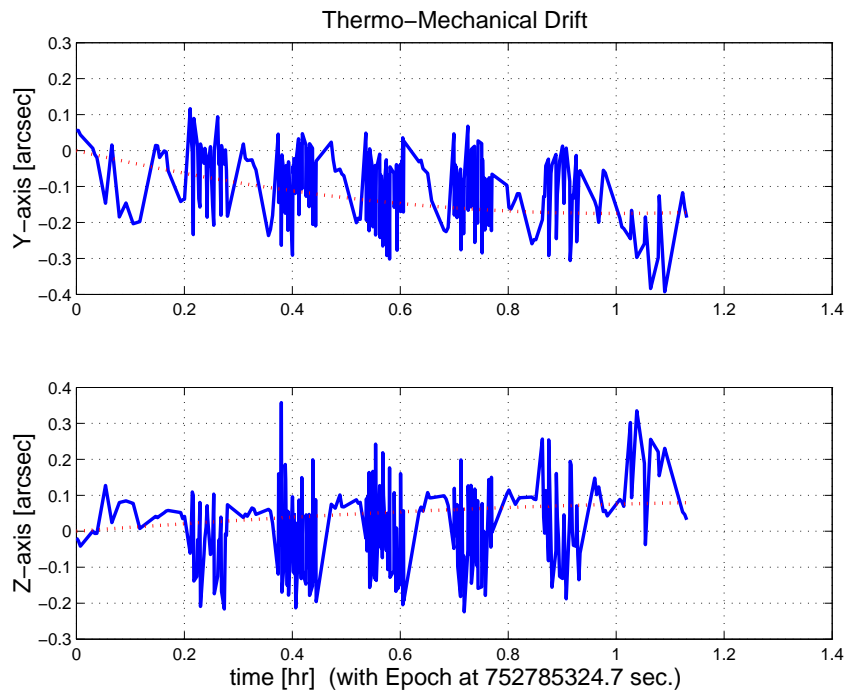


Figure 3.42: Thermo-mechanical boresight drift (equiv. angle in Body frame)

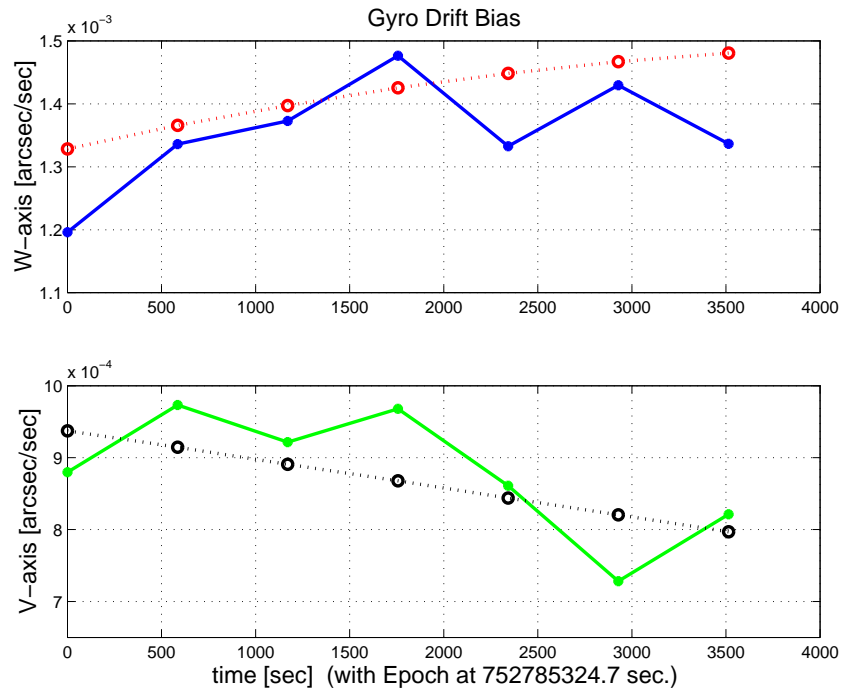


Figure 3.43: Gyro drift bias contribution (equiv. rate in (W,V) coords)

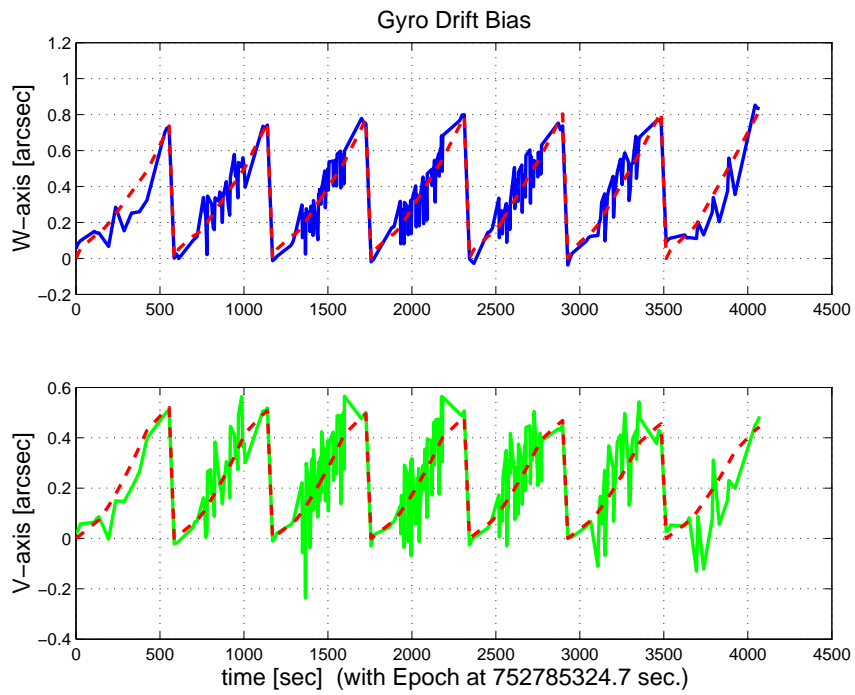


Figure 3.44: Gyro drift bias contribution (equiv. angle in (W,V) coords)

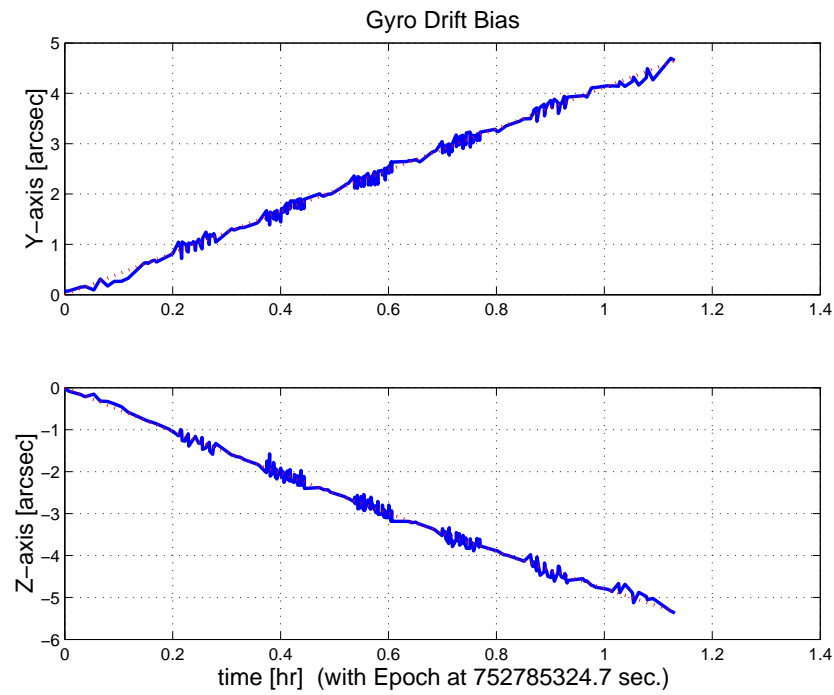


Figure 3.45: Gyro drift bias contribution (equiv. angle in Body frame)

3.2 IPF OUTPUT DATA (IF MINI FILE)

OUTPUT FILE NAME: IFmini502095.dat DATE: 12-Nov-2003 TIME: 17:59
 INSTRUMENT NAME: MIPS_24um_center NF: 95
 IPF FILTER VERSION: IPF.V3.0.OB SW RELEASE DATE: November 3, 2003
 FRAME TABLE USED: BodyFrames_FTU_13a

----- IPF BROWN ANGLE SUMMARY -----

Frame Number	WAS			IS		
	theta_Y (arcmin)	theta_Z (arcmin)	angle (deg)	theta_Y (arcmin)	theta_Z (arcmin)	angle (deg)
095	+6.716105	+4.246060	+0.637930	+6.722262	+4.261820	+0.634863
096	+6.695190	+7.060913	+0.637930	+6.704089	+7.074454	+0.634863
099	+7.756798	+4.259313	+0.637930	+7.763455	+4.275316	+0.634863
100	+5.659609	+4.234140	+0.637930	+5.665413	+4.249600	+0.634863
103	+6.819955	+4.247316	+0.637930	+6.826155	+4.263102	+0.634863
104	+6.633060	+4.245067	+0.637930	+6.639183	+4.260805	+0.634863

OFFSET	NF	Delta_CW	Delta_CV
0	95	+0.000	+0.000 pixels

OFFSET FRAME NAME: MIPS_24um_center

Brown Angle	theta_Y(arcmin)	theta_Z(arcmin)	angle(deg)
WAS(FTB)	+6.716105	+4.246060	+0.637930
IS (EST)	+6.722262	+4.261820	+0.634863
dT_EST	+0.006157	+0.015760	-0.003066
T_sSIGMA	+0.000347	+0.000356	+0.003963
dT_EST/T_sSIGMA	+17.747215	+44.225384	-0.773678

OFFSET	NF	Delta_CW	Delta_CV
1	96	+0.000	-64.000 pixels

OFFSET FRAME NAME: MIPS_24um_plusY_edge

Brown Angle	theta_Y(arcmin)	theta_Z(arcmin)	angle(deg)
WAS(FTB)	+6.695190	+7.060913	+0.637930
IS (EST)	+6.704089	+7.074454	+0.634863
dT_EST	+0.008900	+0.013541	-0.003066
T_sSIGMA	+0.000555	+0.000557	+0.003963
dT_EST/T_sSIGMA	+16.034081	+24.289127	-0.773679

OFFSET	NF	Delta_CW	Delta_CV
2	99	+25.000	+0.000 pixels

OFFSET FRAME NAME: MIPS_24um_small_FOV1

Brown Angle	theta_Y(arcmin)	theta_Z(arcmin)	angle(deg)
WAS(FTB)	+7.756798	+4.259313	+0.637930
IS (EST)	+7.763455	+4.275316	+0.634863
dT_EST	+0.006657	+0.016003	-0.003066
T_sSIGMA	+0.000327	+0.000331	+0.003963
dT_EST/T_sSIGMA	+20.376462	+48.383736	-0.773678

OFFSET	NF	Delta_CW	Delta_CV
3	100	-25.500	+0.000 pixels

OFFSET FRAME NAME: MIPS_24um_small_FOV2

Brown Angle	theta_Y(arcmin)	theta_Z(arcmin)	angle(deg)
WAS(FTB)	+5.659609	+4.234140	+0.637930
IS (EST)	+5.665413	+4.249600	+0.634863
dT_EST	+0.005804	+0.015460	-0.003066
T_sSIGMA	+0.000345	+0.000353	+0.003963
dT_EST/T_sSIGMA	+16.842199	+43.827855	-0.773678

OFFSET	NF	Delta_CW	Delta_CV
4	103	+2.500	+0.000 pixels

OFFSET FRAME NAME: MIPS_24um_large_FOV1

Brown Angle	theta_Y(arcmin)	theta_Z(arcmin)	angle(deg)
WAS(FTB)	+6.819955	+4.247316	+0.637930
IS (EST)	+6.826155	+4.263102	+0.634863

dT_EST	+0.006200	+0.015786	-0.003066	
T_sSIGMA	+0.000346	+0.000355	+0.003963	
dT_EST/T_sSIGMA	+17.923324	+44.461549	-0.773678	
OFFSET	NF	Delta_CW	Delta_CV	
5	104	-2.000	+0.000 pixels	
OFFSET FRAME NAME: MIPS_24um_large_FOV2				
Brown Angle	theta_Y(arcmin)	theta_Z(arcmin)	angle(deg)	
WAS(FTB)	+6.633060	+4.245067	+0.637930	
IS (EST)	+6.639183	+4.260805	+0.634863	
dT_EST	+0.006123	+0.015738	-0.003066	
T_sSIGMA	+0.000348	+0.000357	+0.003963	
dT_EST/T_sSIGMA	+17.620400	+44.067498	-0.773678	
VARNAME	MEAN	SIGMA	SCALED_SIGMA	
a00	-7.1483663598284131E-005	+8.3689018959475799E-005	+6.3454309533093715E-005	
b00	-8.2332613185896113E-005	+1.5397932908284016E-004	+1.1674951063832901E-004	
c00	-1.1898982444093680E-003	+9.2386870244822310E-005	+7.0049155005000202E-005	
a10	+4.3869953922393039E+000	+2.9810513782994280E-001	+2.2602792964303187E-001	
b10	+3.9221961161865524E+000	+4.3953333577647458E-001	+3.3326097838449709E-001	
c10	+1.1192011609559140E+001	+4.1248789450931422E-001	+3.1275470620013202E-001	
d10	-1.2749757840376732E+000	+3.1039075016287149E-001	+2.3534307107341162E-001	
a01	+8.0166656098807962E+000	+1.9038037057210550E-001	+1.4434934371924124E-001	
b01	+4.3408516848575873E+000	+2.6000694788928874E-001	+1.9714129233741992E-001	
c01	-1.6315563575909437E+001	+1.7465848058828171E-001	+1.3242876338645143E-001	
d01	-2.3027667714198565E+000	+2.0041717897153324E-001	+1.5195940719973244E-001	
e01	-1.8615193399323093E+001	+2.7403632194553756E-001	+2.0777858089676884E-001	
f01	+2.4951516451838653E+000	+1.8179535387364951E-001	+1.3784005117759501E-001	
del_alpha	+2.0546020126129688E-012	+1.9445133146356767E-004	+1.4743600927842344E-004	
beta	+9.6352536288366852E-001	+2.9581274582215383E-004	+2.2428980254055180E-004	
del_theta1	-4.1639974346190101E-012	+9.1234215403327608E-005	+6.9175194263120307E-005	
del_theta2	+2.9193241328281187E-015	+1.3309587026726922E-007	+1.0091534892535065E-007	
del_theta3	+1.9103363023019790E-015	+1.3671145890151260E-007	+1.0365674419075229E-007	
del_arx	-1.6358034091640055E-012	+4.0298640674200208E-005	+3.0555053110872764E-005	
del_ary	-8.0731320463576082E-015	+4.1409217179251670E-006	+3.1397109406763152E-006	
del_arz	-1.0678491916166684E-014	+4.1414466083986776E-006	+3.1401089207577074E-006	
brx	+8.6501874527617348E-008	+4.6582667635513882E-008	+3.5319699618565577E-008	
bry	-4.7827819312958814E-010	+5.5718869766715692E-009	+4.2246909486695467E-009	
brz	+1.4902932295557609E-010	+5.5725663867257203E-009	+4.2252060878886698E-009	
crx	-4.4908521250393319E-011	+2.5091404716659140E-011	+1.9024691426744733E-011	
cry	+1.3406296765731100E-013	+3.0629952712414972E-012	+2.3224104244055498E-012	
crz	-2.6709054980262189E-014	+3.0633717347325634E-012	+2.3226958648514655E-012	
bgx	+1.3746826932538458E-006	+6.7035641095216628E-007	+5.0827460671572639E-007	
bgy	+5.586675990219539E-009	+5.6009361342555372E-009	+4.2467164695793003E-009	
bgz	-7.1355959872991202E-009	+5.7026220578126631E-009	+4.3238163107385899E-009	
cgx	-1.0546172106057815E-010	+2.8361637105433982E-010	+2.1504232241328171E-010	
cgy	-2.3822034964107699E-014	+3.0846248761278921E-012	+2.3388103256184488E-012	
cgz	+3.8341341582141489E-013	+3.1052621789370199E-012	+2.3544578480372822E-012	
LSQF RESIDUAL SIGMA SCALE =	+7.5821547823161595E-001			
a_mirror_ipf	a_mirror(1)	a_mirror(2)	a_mirror(3)	
a_mirror_ipf	+0.0000000000000000E+000	+1.2448015275169691E-002	+9.9992252045631480E-001	
a_mirror_tpf	-1.9537263449556940E-003	+1.3703066411584110E-003	+9.9999715260248545E-001	
beta	beta_0	beta	beta_total	
	+2.8047410000000001E-006	+9.6352536288366852E-001	+2.7024390898197034E-006	
qT	qT(1)	qT(2)	qT(3)	qT(4)
FrmTbl:	+5.5663503708387003E-003	-9.8024034448415199E-004	-6.1211659772710003E-004	+9.9998383996226903E-001
Estim:	+5.5395883224368262E-003	-9.8113213042495991E-004	-6.1442995965742416E-004	+9.9998398628017304E-001
DelTheta	deltheta(1)	deltheta(2)	deltheta(3)	[rad]
	-5.3528300116527123E-005	-1.8418953126579479E-006	-4.5640262051653306E-006	
EulAngT	theta(1)	theta(2)	theta(3)	[rad]
Mean	+1.1080452818704994E-002	-1.9554267057993987E-003	-1.2397130645715245E-003	

```

SigmaT      +9.1234215403327608E-005 +1.3309587026726922E-007 +1.3671145890151260E-007
-----
qR          qR(1)                  qR(2)                  qR(3)                  qR(4)
ASFILE:    +7.1069272235035896E-004 +1.2693007010966539E-003 -1.6164845146704465E-004 +9.999892711639404E-001
Estim:     +6.4089116815482035E-004 +1.2707681879379105E-003 -1.6009611081575892E-004 +9.999897438745344E-001
DelThetaR   delthetaR(1)           delthetaR(2)           delthetaR(3)           [rad]
          -1.3960743710156965E-004 +2.9146945816953547E-006 +2.9252056220284665E-006
EulAngR    angR(1)               angR(2)               angR(3)               [rad]
Mean       +1.2813786214027076E-003 +2.5417417144099072E-003 -3.1856407944289076E-004
SigmaR     +4.0298640674200208E-005 +4.1409217179251670E-006 +4.1414466083986776E-006
-----
Initial Gyro Bias      Bg0(1)                  Bg0(2)                  Bg0(3)
          -4.2404289501973835E-007 -2.1017206108808750E-007 +3.7394286778180685E-007
Gyro Bias Correction   Bg(1)                   Bg(2)                   Bg(3)
          +1.3746826932538458E-006 +5.5868675890219539E-009 -7.1355959872991202E-009
Total Gyro Bias        BgT(1)                 BgT(2)                 BgT(3)
          +9.5063979823410742E-007 -2.0458519348906556E-007 +3.6680727179450773E-007
-----
Initial Gyro Bias Rate   Cg0(1)                  Cg0(2)                  Cg0(3)
          +0.0000000000000000E+000 +0.0000000000000000E+000 +0.0000000000000000E+000
Gyro Bias Rate Correction  Cg(1)                   Cg(2)                   Cg(3)
          -1.0546172106057815E-010 -2.3822034964107699E-014 +3.8341341582141489E-013
Total Gyro Bias Rate     CgT(1)                 CgT(2)                 CgT(3)
          -1.0546172106057815E-010 -2.3822034964107699E-014 +3.8341341582141489E-013
-----
OFFSET      NF      Delta_CW      Delta_CV
1          96      +0.000      -64.000      pixels
OFFSET FRAME NAME: MIPS_24um_plusY_edge
qT          qT(1)                  qT(2)                  qT(3)                  qT(4)
WAS(FTB)   +5.5659517308697505E-003 -9.7947717279747932E-004 -1.0215305487940502E-003 +9.9998350850458306E-001
IS (EST)   +5.5391892302457772E-003 -9.8075512205410601E-004 -1.0235190131603232E-003 +9.9998365382184728E-001
-----
DelTheta   deltheta(1)           deltheta(2)           deltheta(3)
Units      rad                  rad                  rad
          -5.3527015441121022E-005 -2.6324891521096876E-006 -3.9098432771071365E-006
EulAngT   theta(1)              theta(2)              theta(3)              [rad]
Mean       +1.1080452818704994E-002 -1.9501404860023971E-003 -2.0578751070514552E-003
sSigmaT    +6.9175172452950074E-005 +1.6145576149548978E-007 +1.6216794635786196E-007
SigmaT     +9.1234186638193088E-005 +2.1294179046839382E-007 +2.1388108132016227E-007
-----
OFFSET      NF      Delta_CW      Delta_CV
2          99      +25.000      +0.000      pixels
OFFSET FRAME NAME: MIPS_24um_small_FOV1
qT          qT(1)                  qT(2)                  qT(3)                  qT(4)
WAS(FTB)   +5.5662538280227556E-003 -1.1316112973882811E-003 -6.1320141015468849E-004 +9.9998367999594084E-001
IS (EST)   +5.5394913486320379E-003 -1.1325760431327120E-003 -6.1555383661802119E-004 +9.9998382606949154E-001
-----
DelTheta   deltheta(1)           deltheta(2)           deltheta(3)
Units      rad                  rad                  rad
          -5.3529847717150147E-005 -1.9882633972898595E-006 -4.6332342969442967E-006
EulAngT   theta(1)              theta(2)              theta(3)              [rad]
Mean       +1.1080452818704995E-002 -2.2582976590658772E-003 -1.2436390435682327E-003
sSigmaT    +6.9175191270559803E-005 +9.5038820303407841E-008 +9.6211995108954678E-008
SigmaT     +9.1234211456480595E-005 +1.2534539722806325E-007 +1.2689268139625647E-007
-----
OFFSET      NF      Delta_CW      Delta_CV
3          100      -25.500      +0.000      pixels
OFFSET FRAME NAME: MIPS_24um_small_FOV2
qT          qT(1)                  qT(2)                  qT(3)                  qT(4)
WAS(FTB)   +5.5664474678460652E-003 -8.2657205344854390E-004 -6.1123845851204566E-004 +9.9998397878604794E-001
IS (EST)   +5.5396858383255053E-003 -8.2741226176116865E-004 -6.1350439704704364E-004 +9.9998412531505554E-001
-----
DelTheta   deltheta(1)           deltheta(2)           deltheta(3)
Units      rad                  rad                  rad
          -5.3526747727956736E-005 -1.7382092459494264E-006 -4.4779840357582723E-006

```

```

EulAngT      theta(1)          theta(2)          theta(3)          [rad]
Mean        +1.1080452818704995E-002 -1.6480017564348270E-003 -1.2361585171670793E-003
sSigmaT     +6.9175190811090575E-005 +1.0023897795076180E-007 +1.0260747136464287E-007
SigmaT      +9.1234210850492923E-005 +1.3220381386113210E-007 +1.3532758735544943E-007
-----
OFFSET      NF    Delta_CW    Delta_CV
4           103   +2.500     +0.000    pixels
OFFSET FRAME NAME: MIPS_24um_large_FOV1
qT          qT(1)          qT(2)          qT(3)          qT(4)
WAS(FTB)   +5.5663407785030133E-003 -9.9534554975494265E-004 -6.1221510359754845E-004 +9.9998382503430572E-001
IS (EST)   +5.539578678573916E-003 -9.9624363394664774E-004 -6.1453270297617769E-004 +9.9998397132961070E-001
DelTheta    deltheta(1)      deltheta(2)      deltheta(3)
Units       rad            rad            rad
EulAngT    theta(1)          theta(2)          theta(3)          [rad]
Mean        +1.1080452818704994E-002 -1.9856481312776494E-003 -1.2400860082130928E-003
sSigmaT     +6.9175194249526784E-005 +1.0062450505766215E-007 +1.0328015246073062E-007
SigmaT      +9.1234215385399296E-005 +1.3271228027730116E-007 +1.3621477723141535E-007
-----
OFFSET      NF    Delta_CW    Delta_CV
5           104   -2.000     +0.000    pixels
OFFSET FRAME NAME: MIPS_24um_large_FOV2
qT          qT(1)          qT(2)          qT(3)          qT(4)
WAS(FTB)   +5.5663580350760848E-003 -9.6816128275258886E-004 -6.1203938908990752E-004 +9.9998385173448789E-001
IS (EST)   +5.5395960203246143E-003 -9.6904818972953213E-004 -6.1434930810243499E-004 +9.9998399807020177E-001
DelTheta    deltheta(1)      deltheta(2)      deltheta(3)
Units       rad            rad            rad
EulAngT    theta(1)          theta(2)          theta(3)          [rad]
Mean        +1.1080452818704995E-002 -1.9312600727366489E-003 -1.2394178543374728E-003
sSigmaT     +6.9175194228527482E-005 +1.010895896764583E-007 +1.0388531283190961E-007
SigmaT      +9.1234215357703609E-005 +1.3332567399364733E-007 +1.3701291494892859E-007
-----
q(1)          q(2)          q(3)          q(4)
PCRS1A: +5.3371888965461637E-007 +3.7444233778550031E-004 -1.4253684912431913E-003 +9.9999891405806784E-001
PCRS2A: -5.2779261998836216E-007 +3.8462959425181312E-004 +1.3722087221825403E-003 +9.9999898455099423E-001
*****
CS-FILE PARAMETERS: ***** AS-FILE PARAMETERS: *****
Row (01) PIX2RADX: +1.2087416876100000E-005 Row (1) TASTART: +7.5278450049075317E+008
Row (02) PIX2RADY: +1.2595908372599999E-005 Row (2) TASTOP: +7.5279000039073789E+008
Row (03) CX0:      +6.4500000000000000E+001 Row (3) S/C TIME: +7.5278198529074097E+008
Row (04) CY0:      +6.4500000000000000E+001 Row (4) QR1:      +7.1069272235035896E-004
Row (05) BETA0:    +2.8047410000000001E-006 Row (5) QR2:      +1.2693007010966539E-003
Row (06) GAMMA_E0: +2.0070000000000000E+003 Row (6) QR3:      -1.6164845146704465E-004
Row (07) D11:      -1.0000000000000000E+000 Row (7) QR4:      +9.9999892711639404E-001
Row (08) D12:      +0.0000000000000000E+000
Row (09) D21:      +0.0000000000000000E+000
Row (10) D22:      -1.0000000000000000E+000
Row (11) DG:       -1.0000000000000000E+000
-----
INITIAL STA-TO-PCRS ALIGNMENT (R) KNOWLEDGE (1-SIGMA)
SIGMA(X)      SIGMA(Y)      SIGMA(Z)
5.12047425E+000 3.93765904E-001 3.93994671E-001 [arcsec]
-----
PIX2RADX = 1.208741687610E-005[rad/pixel]
XPIXSIZE = 2.4932[arcsec]
PIX2RADY = 1.259590837260E-005[rad/pixel]
YPIXSIZE = 2.5981[arcsec]
CX0 = 64.5[pixel] = 160.81[arcsec]
CY0 = 64.5[pixel] = 167.58[arcsec]
-----
NOMINAL BETA0 = 2.804741000000E-006[rad/encoder unit]

```

```

ENCODER UNIT SIZE = 0.58[arcsec]
GAMMA_E0 = 2007.00[encoder unit] = 1161.09[arcsec]
-----
| -1 | +0 |
FLIP MATRIX D = |----|----| and DG = -1
| +0 | -1 |
-----

```

3.3 IPF EXECUTION LOG

```

*****
IPF EXECUTION-LOG FILE NAME: LG502095.dat
INSTRUMENT TYPE: MIPS_24um_center
IPF FILTER EXECUTION DATE: 12-Nov-2003 TIME: 17:56
IPF FILTER VERSION USED: IPF.V3.0.OB
*****


----- Loading & Preparing Input Files -----
AAFILE: AA501095 Loaded! AAFILE dimension = 55000 X 21
ASFILE: AS501095 Loaded!
CAFILe: CA502095 Loaded! CAFILe dimension = 214 X 15
CBFILE: CB501095 Loaded! CBFILE dimension = 63 X 15
CCFILE: CC502095 Created! CCFILE dimension = 277 X 19
CSFILE: CS501095 Loaded!
Loading Input Files Completed!
-----


----- Selected Mask Vectors -----
index = 1 2 3 4 5 6 7 8 9 10 11 12 13 14 15 16 17 18 19 20
-----
mask1 = [ 1 1 1 1 1 1 1 0 0 0 0 1 1 1 1 1 1 1 ]
mask2 = [ 1 1 1 1 1 1 1 1 1 1 1 1 1 1 1 1 1 1 ]
-----


----- Selected Initial Gyro Bias Parameters -----
User Entered 1 : Use AFILe database - from S/C filter
IPF Linearized Using Nominal Gyro Bias Estimates
bg0 = [-4.2404289501973835E-007 -2.1017206108808750E-007 +3.7394286778180685E-007 ]
cg0 = [+0.000000000000000E+000 +0.000000000000000E+000 +0.000000000000000E+000 ]
-----


----- Gyro Pre-Processor Run Completed -----
AGFILE CREATED: AG502095.m ACFILE CREATED: AC502095.m
-----
Total Gyro Preprocessor Execution Time: 30 seconds

FRAME TABLE ENTRIES FOR PCRS LOADED TO TPCRS
q_PCRS4 = [ +5.3371888965461637E-007 q_PCRS5 = [ +7.3379987833742897E-007
            +3.7444233778550031E-004 +5.2236196154513707E-004
            -1.4253684912431913E-003 -1.4047712280184723E-003
            +9.9999891405806784E-001 ]; +9.9999887687698918E-001 ];
q_PCRS8 = [ -5.2779261998836216E-007 q_PCRS9 = [ -7.1963421681856818E-007
            +3.8462959425181312E-004 +5.3239763239987400E-004
            +1.3722087221825403E-003 +1.3516841804518383E-003
            +9.9999898455099423E-001 ]; +9.9999894475050310E-001 ];
----- Initial Conditions for State ----- ----- Initial Square-Root Cov (diag) -----
p1(01) = a00 = +0.000000000000000E+000 Sigma_initial(01,01) = 1.000000000000000E+000
p1(02) = b00 = +0.000000000000000E+000 Sigma_initial(02,02) = 1.000000000000000E+000
p1(03) = c00 = +0.000000000000000E+000 Sigma_initial(03,03) = 1.000000000000000E+000
-----
```

```

p1(04) = a10 = +0.0000000000000000E+000 Sigma_initial(04,04) = 1.0000000000000000E+002
p1(05) = b10 = +0.0000000000000000E+000 Sigma_initial(05,05) = 1.0000000000000000E+002
p1(06) = c10 = +0.0000000000000000E+000 Sigma_initial(06,06) = 1.0000000000000000E+002
p1(07) = d10 = +0.0000000000000000E+000 Sigma_initial(07,07) = 1.0000000000000000E+002
p1(08) = a20 = +0.0000000000000000E+000 Sigma_initial(08,08) = 9.9999000000000000E+004
p1(09) = b20 = +0.0000000000000000E+000 Sigma_initial(09,09) = 9.9999000000000000E+004
p1(10) = c20 = +0.0000000000000000E+000 Sigma_initial(10,10) = 9.9999000000000000E+004
p1(11) = d20 = +0.0000000000000000E+000 Sigma_initial(11,11) = 9.9999000000000000E+004
p1(12) = a01 = +0.0000000000000000E+000 Sigma_initial(12,12) = 1.0000000000000000E+004
p1(13) = b01 = +0.0000000000000000E+000 Sigma_initial(13,13) = 1.0000000000000000E+004
p1(14) = c01 = +0.0000000000000000E+000 Sigma_initial(14,14) = 1.0000000000000000E+004
p1(15) = d01 = +0.0000000000000000E+000 Sigma_initial(15,15) = 1.0000000000000000E+004
p1(16) = e01 = +0.0000000000000000E+000 Sigma_initial(16,16) = 1.0000000000000000E+004
p1(17) = f01 = +0.0000000000000000E+000 Sigma_initial(17,17) = 1.0000000000000000E+004
-----
p2f(01) = am1 = +0.0000000000000000E+000 Sigma_initial(18,18) = 1.0000000000000001E-001
p2f(02) = am2 = +0.0000000000000000E+000 Sigma_initial(19,19) = 1.0000000000000001E-001
p2f(03) = am3 = +1.0000000000000000E+000 Sigma_initial(20,20) = 1.0000000000000001E-001
p2f(04) = beta = +1.0000000000000000E+000 Sigma_initial(21,21) = 1.0000000000000000E-002
p2f(05) = qT1 = +5.5663503708387055E-003 Sigma_initial(22,22) = 1.0000000000000000E-002
p2f(06) = qT2 = -9.8024034448415285E-004 Sigma_initial(23,23) = 2.4824759709670297E-004
p2f(07) = aT3 = -6.1211659772710057E-004 Sigma_initial(24,24) = 1.9090309734073366E-005
p2f(08) = qT4 = +9.9998383996226992E-001 Sigma_initial(25,25) = 1.9101400670094249E-005
p2f(09) = qR1 = +7.1069272235035896E-004 Sigma_initial(26,26) = 2.4569421138237143E-004
p2f(10) = qR2 = +1.2693007010966539E-003 Sigma_initial(27,27) = 2.4569421138237143E-004
p2f(11) = qR3 = -1.6164845146704465E-004 Sigma_initial(28,28) = 2.4569421138237143E-004
p2f(12) = qR4 = +9.9999892711639404E-001 Sigma_initial(29,29) = 6.0365645506805417E-008
p2f(13) = brx = +0.0000000000000000E+000 Sigma_initial(30,30) = 6.0365645506805417E-008
p2f(14) = bry = +0.0000000000000000E+000 Sigma_initial(31,31) = 6.0365645506805417E-008
p2f(15) = brz = +0.0000000000000000E+000 Sigma_initial(32,32) = 2.4569421138237143E-004
p2f(16) = crx = +0.0000000000000000E+000 Sigma_initial(33,33) = 2.4569421138237143E-004
p2f(17) = cry = +0.0000000000000000E+000 Sigma_initial(34,34) = 2.4569421138237143E-004
p2f(18) = crz = +0.0000000000000000E+000 Sigma_initial(35,35) = 6.0365645506805417E-008
p2f(19) = bgx = +0.0000000000000000E+000 Sigma_initial(36,36) = 6.0365645506805417E-008
p2f(20) = bgy = +0.0000000000000000E+000 Sigma_initial(37,37) = 6.0365645506805417E-008
p2f(21) = bgz = +0.0000000000000000E+000
p2f(22) = cgx = +0.0000000000000000E+000
p2f(23) = cgy = +0.0000000000000000E+000
p2f(24) = cgz = +0.0000000000000000E+000
-----
```

```

----- IPF KALMAN FILTER STARTED -----
Iteration#001: |dp|= +2.952094920438E+001 RMS(|Res|)=+1.360804785282E-005
Iteration#002: |dp|= +3.491840911489E-002 RMS(|Res|)=+3.187467791596E-006
Iteration#003: |dp|= +9.217527314400E-003 RMS(|Res|)=+7.561420194326E-007
Iteration#004: |dp|= +1.074596686390E-003 RMS(|Res|)=+7.460469974737E-007
Iteration#005: |dp|= +1.741280816550E-004 RMS(|Res|)=+7.462230885838E-007
Iteration#006: |dp|= +3.810899857049E-005 RMS(|Res|)=+7.462031809734E-007
Iteration#007: |dp|= +2.456510914864E-006 RMS(|Res|)=+7.461937228395E-007
Iteration#008: |dp|= +1.164877261324E-006 RMS(|Res|)=+7.461936082887E-007
Iteration#009: |dp|= +7.029527770513E-009 RMS(|Res|)=+7.461940158476E-007
Iteration#010: |dp|= +3.222891111630E-008 RMS(|Res|)=+7.461940615551E-007
Iteration#011: |dp|= +2.450075153912E-009 RMS(|Res|)=+7.461940470980E-007
Iteration#012: |dp|= +5.693237564147E-009 RMS(|Res|)=+7.461940437955E-007
Iteration#013: |dp|= +5.930209600436E-009 RMS(|Res|)=+7.461940440499E-007
Iteration#014: |dp|= +4.284057305407E-009 RMS(|Res|)=+7.461940442074E-007
Iteration#015: |dp|= +3.44328577238E-009 RMS(|Res|)=+7.461940442106E-007
Iteration#016: |dp|= +1.012345600230E-008 RMS(|Res|)=+7.461940440253E-007
Iteration#017: |dp|= +5.306406906374E-009 RMS(|Res|)=+7.461940447513E-007
Iteration#018: |dp|= +2.657906037575E-009 RMS(|Res|)=+7.461940444398E-007
Iteration#019: |dp|= +3.134069682581E-009 RMS(|Res|)=+7.461940443569E-007
Iteration#020: |dp|= +7.952212488353E-009 RMS(|Res|)=+7.461940442511E-007
Iteration#021: |dp|= +1.297088392375E-008 RMS(|Res|)=+7.461940447672E-007
Iteration#022: |dp|= +4.113643274019E-009 RMS(|Res|)=+7.461940443220E-007
Iteration#023: |dp|= +2.267951716831E-009 RMS(|Res|)=+7.461940442380E-007
Iteration#024: |dp|= +1.064565888578E-008 RMS(|Res|)=+7.461940441719E-007
Iteration#025: |dp|= +1.069122481073E-008 RMS(|Res|)=+7.461940443310E-007
IPF Kalman Filter Completed with Error |dp1| + |dp2| = +1.0691224810727679E-008
```

----- IPF LEAST SQUARES FILTER STARTED -----

```

Iteration#001 COND#=+3.656560787516E+009, |dp|=+2.952162261542E+001
Iteration#002 COND#=+3.656548220846E+009, |dp|=+2.799068449583E-002
Iteration#003 COND#=+3.656536384546E+009, |dp|=+1.102819963152E-003
Iteration#004 COND#=+3.656536398216E+009, |dp|=+2.735596513005E-005
Iteration#005 COND#=+3.656536468954E+009, |dp|=+3.592892405011E-007
Iteration#006 COND#=+3.656536241406E+009, |dp|=+4.467855011069E-009
Iteration#007 COND#=+3.656536289022E+009, |dp|=+1.295784239013E-010
Iteration#008 COND#=+3.656536293539E+009, |dp|=+9.602507634554E-011
Iteration#009 COND#=+3.656536347214E+009, |dp|=+6.940640496536E-011
Iteration#010 COND#=+3.656536288296E+009, |dp|=+7.408830630610E-011
Iteration#011 COND#=+3.656536262915E+009, |dp|=+5.827006391768E-011
Iteration#012 COND#=+3.656536220430E+009, |dp|=+8.412511383992E-011
Iteration#013 COND#=+3.656536266482E+009, |dp|=+9.909832341214E-011
Iteration#014 COND#=+3.656536337751E+009, |dp|=+1.293991841449E-010
Iteration#015 COND#=+3.656536276125E+009, |dp|=+9.493737064148E-011
Iteration#016 COND#=+3.656536191140E+009, |dp|=+7.564611301899E-011
Iteration#017 COND#=+3.656536363557E+009, |dp|=+7.685464774247E-011
Iteration#018 COND#=+3.656536375019E+009, |dp|=+6.443684635532E-011
Iteration#019 COND#=+3.656536289051E+009, |dp|=+8.667488921141E-011
Iteration#020 COND#=+3.656536297495E+009, |dp|=+8.016624546160E-011
Iteration#021 COND#=+3.656536296862E+009, |dp|=+9.111290534841E-011
Iteration#022 COND#=+3.656536312004E+009, |dp|=+5.851009233291E-011
Iteration#023 COND#=+3.656536309298E+009, |dp|=+5.154955056536E-011
Iteration#024 COND#=+3.656536266998E+009, |dp|=+7.550650772837E-011
Iteration#025 COND#=+3.656536172379E+009, |dp|=+7.692711241865E-011
IPF Least Squares Filter Completed with Error |dp1| + |dp2| = +7.6927112418647572E-011
-----
```

Total Execution Time: 167 seconds

4 COMMENTS

Overall the data looked clean, and the filter converged nicely.

Comments:

1. The run was performed in normal IPF operating mode.
2. This run uses IPF version 3.0 where the gyro drift bias estimates make use of the recently corrected GCF signs, (MCR 2521) and now show no sandwich-to-sandwich variations.
3. There were 7 sandwich maneuvers with 214 science centroids (4 centroids were removed from the original 218 centroids, at the 3-sigma level) and 63 PCRS measurements.
4. We estimated 33 parameters consisting of: 3 constant and 6 linear plate scales, 4 Gamma Dependent parameters, 2 mirror parameters, 3 IPF alignment angles, 3 STA-to-PCRS alignment angles, 6 STA-to-PCRS thermomechanical drift parameters, and 3 gyro bias and 3 gyro bias-drift parameters.
5. The linear plate scales were helpful in this run to estimate centroids accurately (see quiver plots in Figures 3-33 and 3-34). The constant plate scales were much smaller than the linear terms. The estimated plate scales (constant and linaer) are consistent with those obtained earlier from the Coarse Focal Plane Survey results.
6. The scan mirror parameter estimates indicate that the mirror spin axis is tilted by 0.7 deg and the scan mirror scale factors are off by 4 percent. These values are consistent with those obtained earlier from the Coarse Focal Plane Survey results.

We recommend updating frames 95, 96, 99, 100, 103 and 104 with the new quaternions listed in the IF file IF502095.dat. This contains adjustments of 0.37 and 0.95 arcseconds in Y and Z, and .003 deg in twist (for the prime frame). In our best judgement, this fine survey is accurate to 0.091 arcsecond which satisfies its fine survey requirement of 0.14 arcseconds by a good margin.

IPF TEAM CONTACT INFORMATION

IPF Team email	ipf@sirtfweb.jpl.nasa.gov	
David S. Bayard	X4-8208	David.S.Bayard@jpl.nasa.gov (TEAM LEADER)
Dhemetrio Boussalis	X4-3977	boussali@grover.jpl.nasa.gov
Paul Brugarolas	X4-9243	Paul.Brugarolas@jpl.nasa.gov
Bryan H. Kang	X4-0541	Bryan.H.Kang@jpl.nasa.gov
Edward.C.Wong	X4-3053	Edward.C.Wong@jpl.nasa.gov (TASK MANAGER)

ACKNOWLEDGEMENTS

This work was performed at the Jet Propulsion Laboratory, California Institute of Technology, under contract with the National Aeronautics and Space Administration.

References

- [1] D.S. Bayard, B.H. Kang, *SIRTF Instrument Pointing Frame Kalman Filter Algorithm*, JPL D-Document D-24809, September 30, 2003.
- [2] B.H. Kang, D.S. Bayard, *SIRTF Instrument Pointing Frame (IPF) Software Description Document and User's Guide*, JPL D-Document D-24808, September 30, 2003.
- [3] D.S. Bayard, B.H. Kang, *SIRTF Instrument Pointing Frame (IPF) Kalman Filter Unit Test Report*, JPL D-Document D-24810, September 30, 2003.
- [4] *Space Infrared Telescope Facility In-Orbit Checkout and Science Verification Mission Plan*, JPL D-Document D-22622, 674-FE-301 Version 1.4, February 8, 2002.
- [5] *Space Infrared Telescope Facility Observatory Description Document*, Lockheed Martin LMMS/P458569, 674-SEIT-300 Version 1.2, November 1, 2002.
- [6] *SIRTF Software Interface Specification for Science Centroid INPUT Files (CAFILER, CSFILE)*, JPL SOS-SIS-2002, November 18, 2002.
- [7] *SIRTF Software Interface Specification for Inferred Frames Offset INPUT Files (OFILE)*, JPL SOS-SIS-2003, November 18, 2002.
- [8] *SIRTF Software Interface Specification for PCRS Centroid INPUT Files (CBFILE)*, JPL SIS-FES-015, November 18, 2002.
- [9] *SIRTF Software Interface Specification for Attitude INPUT Files (AFILE, ASFILE)*, JPL SIS-FES-014, January 7, 2002.
- [10] *SIRTF Software Interface Specification for IPF Filter Output Files (IFFILE, LGFILE, TARFILE)*, JPL SOS-SIS-2005, November 18, 2002.
- [11] R.J. Brown, *Focal Surface to Object Space Field of View Conversion*. Systems Engineering Report SER No. S20447-OPT-051, Ball Aerospace & Technologies Corp., November 23, 1999.